SLAC-PUB-3263
November 1983
(T/E)

APPLIED CHROMODYNAMICS*

STANLEY J. BRODSKY

Stanford Linear Accelerator Center

Stanford University, Stanford, California 94305

A number of novel features of QCD are reviewed, including the consequences of formation zone and color transparency phenomena in hadronic collisions, the use of automatic scale setting for perturbative predictions, null-zone phenomena as a fundamental test of gauge theory, and the relationship of intrinsic heavy colored particle Fock state components to new particle production. We conclude with a review of the applications of QCD to nuclear multiquark systems.

Invited lectures presented at the XXIII Cracow School of Theoretical Physics: Fundamental Interactions and Structure of Matter, Zakopane, Poland, 29 May to 11 June, 1983, to be published in Acta Physica Polonica.

* Work supported by the Department of Energy, contract DE-AC03-76SF00515.

1. Introduction

Although precise quantitative tests are still lacking, it appears that quantum chromodynamics (QCD) is the fundamental theory of strong and nuclear phenomena in the same sense that quantum electrodynamics gives a fundamental description of electrodynamic phenomena. QCD provides natural explanations for the basic features of hadronic physics: the meson and baryon spectra, quark statistics, the structure of the weak and electromagnetic currents of hadrons, the scale-invariance of hadronic interactions at short distances, and evidently, color (i.e., quark and gluon) confinement at large distances [1].

Recent determinations of $\Lambda_{\overline{MS}}$, the basic scale of QCD, yield values of order 100 ± 50 MeV (see section 4.1), so that the range of useful perturbative QCD predictions can evidentally be extended to relatively low momentum transfer. Factorization theorems imply that all of the effects of nonperturbative bound state dynamics and collinear singularities can be isolated at momentum transfer Q in terms of process-independent structure functions $G_{i/H}(x,Q)$ and fragmentation functions $D_{H/i}(z,Q)$—or in the case of exclusive processes—distribution amplitudes $\phi_H(x_i,Q)$. Thus, even though of explicit solutions to the bound state problem are not yet known, the arena of QCD tests can be extended to a large domain of inclusive, semi-inclusive, and exclusive processes. Reviews of the applications of QCD to exclusive process, including two-photon processes, are given in reference [2]. In many important phenomenological cases, the same formalism gives normalized predictions for several types of power-law suppressed (higher twist) contributions to inclusive reactions such as "direct" hadron reactions. A review of such processes is given in reference [3].

In these lectures we will focus on a number of applications of QCD outside the domain of e^+e^-, deep-inelastic lepton scattering, and jet tests. We begin with a review in section 2 of recent progress in proving the standard factorization ansatz for high momentum transfer inclusive processes. The ansatz, which is now verified to two loops in perturbation theory for massive lepton pair production [4, 5, 6], is nontrivial because of the transverse momentum smearing and the possibility of color corrections induced by initial state interactions. The physical principles which underlie factorization are emphasized. As we shall discuss in section 2, a necessary condition [4] for the validity of factorization in inclusive reactions is

that the energies of each particle participating in the subprocesses must be large compared to the (rest frame) length of the target. In the case of exclusive processes, the factorization of hadronic amplitudes at large momentum transfer in the form of distribution amplitudes convoluted with hard scattering quark-gluon subprocess amplitudes can be demonstrated systematically to all orders in $\alpha_s(Q^2)$ [7].

An important way to check quantum chromodynamics is to test its novel predictions — especially effects unique to local gauge theory. In section 3, a number of unusual or unexpected aspects of QCD are discussed. These include: "null zone" phenomena — zeroes in the cross section for photon emission in certain kinematic regions unique to gauge theory; "color transparency" phenomena — the small value of interaction cross sections for specific components of hadronic wavefunctions; "formation zone" phenomena — the suppression of inelastic interactions at high energies in targets of fixed length; and "intrinsic charm" — the unusual kinematical effect of virtual charm and other heavy colored components in the wavefunctions of ordinary hadrons.

One of the most interesting problems in hadron physics is the application of quantum chromodynamics [8] (QCD) to multiquark systems, i.e., nuclei. If QCD is correct, then it must provide a fundamental description of nuclear forces and dynamics [9]. QCD provides new—in some cases, dramatic—perspectives to nuclear physics, especially in the high momentum transfer domain ($Q > 1$ GeV) where quark and gluon degrees of freedom and "hidden color" wavefunction components are essential. These applications include corrections to nucleon additivity of nuclear structure functions (the EMC effect) [10], possible connections to the anomalon effect [11], calculations of nuclear amplitudes at large momentum transfer (e.g., the deuteron form factor); the application of "reduced" nuclear amplitudes, which are defined to remove the effects of nucleon compositeness in a covariant fashion; evolution equations for nuclear wavefunctions—e.g., the deuteron six-quark wavefunction evolves to a state which is 80% hidden color at small internucleon separation. Many traditional concepts of standard nuclear physics phenomenology (e.g., the impulse approximation to nuclear form factors, point-like nucleon pair and meson-exchange current contributions to electromagnetic nuclear amplitudes, local meson-nucleon field theory, and the local potential Dirac equation

description of relativistic nucleons), require substantial modification. Conversely, the nucleus provides an important tool for studying central problems of particle physics, such as the evolution of quark and gluon jets in nuclear matter, as well as color transparency and formation zone phenomena. A discussion of these topics is given in section 4.

Finally in the Appendix we discuss a procedure [12] for automatically determining the correct scale for the argument of the running coupling constant and thus eliminating one of the main ambiguities in applying perturbative QCD.

2. Factorization for high momentum transfer inclusive reactions: physical principles [13]

One of the most important problems in perturbative QCD in the last two years has been to understand the validity of the standard factorization ansatz for hadron-hadron induced inclusive reactions. Although factorization is an implicit property of parton models, the existence of diagrams with color exchanging initial state interactions at the leading twist level has made the general proof of factorization in QCD highly problematical [4].

To see the main difficulties from a physical perspective, consider the usual form assumed for massive lepton pair production [see fig. 1(a)]

$$\frac{d\sigma}{dx_1 dx_2}(H_A H_B \to \ell\bar{\ell}X) = \frac{1}{3}\frac{4\pi\alpha^2}{3Q^2}\sum_i Q_i^2\Big[q_A^{(1)}(x_i,Q)\,\bar{q}_B^{(2)}(x_2,Q) + (1\to 2)\Big] \qquad (1)$$

The factorization ansatz identifies the Q^2-evolved quark distributions q_A and $\bar{q}_B$ with those measured in deep inelastic lepton scattering on H_A and H_B. However, for very long targets the initial-state hadronic interactions occurring before the $q\bar{q} \to \ell\bar{\ell}$ annihilation certainly lead to induced radiation and energy loss, secondary beam production, transverse momentum fluctuations, et cetera – i.e.: a profound modification of the incoming hadronic state [see fig. 1(b)]. Since the structure functions associated with deep inelastic neutrino scattering are essentially additive in quark number even for macroscopic targets, eq. (1) can obviously not be valid in general. At the least, an explicit condition related to target length must occur. The original proofs of factorization in QCD for the Drell-Yan process ignored the (Glauber) singularities associated with initial state interactions and thus had no length condition.

The potential problems and complications associated with "wee parton" exchange in the initial state were first mentioned by Drell and Yan in their original work [14]. Collins and Soper [15] have noted that proofs of factorization for hadron pair production in $e^+e^- \to H_A H_B X$ could not be readily extended to $H_A H_B \to \ell\bar{\ell} X$ because of the complications of initial state effects. Possible complications associated with nonperturbative interaction effects were also discussed by Ellis *et al.* [16] Bodwin, Lepage, and I [4] considered the effects of initial state interactions as given by perturbative QCD and showed that specific graphs such as those in fig. 2 lead to color exchange correlations as well as $k_\perp$ fluctuations. We also showed that induced hard collinear gluon radiation is indeed suppressed for incident energies large compared to a scale proportional to the length of the target. More recently, the question of the existence of color correlations on perturbative QCD has been addressed systematically to two loop order by Lindsay *et al.* [5] and also by Bodwin *et al.*, [4]. One finds that because of unitarity and local gauge invariance to two loop order the factorization theorem for $d\sigma/dQ^2\,dx_L$ is correct when applied at high energies to color singlet incident hadrons; more general proofs beyond two loop order await further work [6]. We discuss the progress in this area at the end of this section.

In addition to the above initial state interaction there are additional potential infrared problems in the non-Abelian theory associated with the breakdown of the usual Bloch-Nordsiek cancellation for soft gluon radiation. The work of reference 17 shows that any observable effect is suppressed by powers of s at high energies, again to at least two-loop order.

In addition to these problems the high transverse momentum virtual gluon corrections to the $q\bar{q} \to \ell\bar{\ell}$ vertex lead to relatively large radiative corrections of relative order $\pi^2 C_F(\alpha_s(Q^2)/\pi)$ [18]. It is usually assumed that such corrections exponentiate. As in the case of the $\Upsilon \to 3g$ problem, these corrections spoil the convergence of the perturbation theory and cannot be eliminated by choice of scale or scheme [12].

A remarkable feature of the QCD calculation is the fact that factorization is not destroyed by induced radiation in the target for sufficiently high energy beams. This can be understood in terms of the "formation zone" principle of Landau and Pomeranchuk [19]: a

system does not alter its state for times short compared to its natural scale in its rest frame. More specifically for QCD (in the Glauber/classical scattering region), consider the diagrams for induced radiation for quark-pion scattering shown in fig. 2(b). Here $\ell^{\pm} = \ell^0 \pm \ell^3$, $y = \ell^+/p_B^+$, $x_a = p_a^-/p_A^-$ are the usual light-cone variables. The Feynman propagators of the line before and after radiation are proportional to $y - y_1 + i\epsilon$ and $y - y_2 + i\epsilon$, where the difference of the pole contributions is $y_1 - y_2 = \mathcal{M}^2/x_a s$, and $\mathcal{M}^2$ is the mass of the quark-gluon pair after bremsstrahlung. Using partial fractions, the gluon emission amplitude is then

proportional to

$$\int_0^1 dy\ \psi[(x_b - y)M_n L] \left[\frac{1}{y - y_1 + i\epsilon} - \frac{1}{y - y_2 + i\epsilon}\right] \tag{2}$$

where we have indicated the dependence on the target wave function on target length. The two poles thus cancel in the amplitude if $(\mathcal{M}^2/x_a s)\, M_N L \ll 1$; i.e. the radiation from the two Glauber processes destructively interfere and cancel for quark energies large compared to the target length. If we take $\mathcal{M}^2 \sim \mu^2$ finite, then since $Q^2 = x_a x_b s$, the condition for no induced radiation translates to

$$Q^2 \gg x_b M_N L \mu^2\ . \tag{3}$$

Taking $\mu^2 \sim 0.1\ GeV^2$, this is $Q^2 \gg x_b(0.25\ GeV^2)\, A^{2/3}$; thus one requires $Q^2 \gg x_b(10\ GeV^2)$ to eliminate induced radiation in Uranium targets.

Equation (3) is a new necessary condition for QCD factorization; it is also a prediction that a new type of nuclear shadowing occurs for low Q^2 lepton-pair production. If this condition is not met then the cancellations found in reference 4, for example, fail. The same length condition affects all sources of hard collinear radiation induced by initial or final state interactions of the hadrons or quarks in a nucleus; i.e., effectively hard collinear radiation occurs outside the target at high energies. In particular, fast hadron production from jet fragmentation in $\ell p \to \ell HX$ occurs outside the target. In the case of very long or macroscopic targets, induced radiation destroys any semblance of factorization.

Although induced hard collinear radiation cancels at high energies, the basic processes of $k_\perp$ fluctuations from elastic collisions and induced central radiation [e.g., fig. 2(a) with

$j_z \sim m^2/\sqrt{s}$ in the CM] do remain. One expects that the main effects of initial state interactions can be represented by an eikonal picture where the hadronic wave functions are modified by a phase in impact space (see fig. 3):

$$\psi_A(x_a, \vec{z}_{a\perp})\psi_B(x_b, \vec{z}_{\perp b}) \to \psi_A(x_a, \vec{z}_{a\perp})\psi_B(x_a, \vec{z}_{b\perp})U(\vec{z}_{\perp i}) \,. \tag{4}$$

Here

$$U(\vec{z}_{\perp b}) = P_T \exp\left\{-i \int_{-\infty}^{0} d\tau \, H_I(z_\perp, \tau)\right\} \tag{5}$$

includes elastic and soft inelastic collisions which occur up to the time $\tau = 0$ of the $q\bar{q}$ annihilation. The eikonal leads to an increased transverse smearing of the lepton pair and increased associated radiation in the central region proportional to the number of collisions ($A^{1/3}$) of the quark in the target. For a nucleus we thus predict

$$\Delta\langle Q_\perp^2 \rangle \propto A^{1/3} \,, \quad \Delta \frac{dN}{dy} \propto A^{1/3} \tag{6}$$

In the case of an Abelian gauge theory the integrated cross section

$$\int \frac{d\sigma}{dQ^2 \, dx_L \, d^2Q_\perp} = \frac{d\sigma}{dQ^2 dx_L} \tag{7}$$

in unchanged because of unitarity, $U^\dagger(z_\perp)\, U(z_\perp) = 1$. See fig. 3(b). Thus for an Abelian theory, the increased production at large $Q_\perp$ from initial state interactions must be compensated by a depletion at low $Q_\perp$.

In general, initial state interactions will have a strong modifying effect on all hadron-hadron cross sections which produce particles at large transverse momentum simply because of the $k_\perp$ smearing of very rapidly falling distributions. The initial state exchange interactions combine with the quark and gluon $k_\perp$ distributions intrinsic to the hadron wave functions as well as that induced by the radiation associated with QCD evolution to yield the total $k_\perp$ smearing effect. The unitarity structure of the initial state eikonal interactions provides a finite theory of $k_\perp$ fluctuations even when the hard scattering amplitude is singular at zero momentum transfer.

In a non-Abelian theory the eikonal unitary matrix $U(z_\perp)$ associated with the initial state interactions is a path-color-ordered exponential integrated over the paths of the incident

constituents. Since U is a color matrix it would not be expected to commute with the Drell-Yan $q\bar{q} \to \ell\bar{\ell}$ matrix element

$$U^\dagger M_{DY}^\dagger M_{DY} U \neq M_{DY}^\dagger M_{DY} \, . \tag{8}$$

Thus unless U is effectively diagonal in color, the usual color factor $1/n_c$ in $d\sigma(q\bar{q} \to \ell\bar{\ell})$ would be expected to be modified. In principle, this effect could change the usual color factor $1/n_c$ to n_c or event to 0 without violating unitarity, although, as shown by Mueller [20], the deviation from $1/n_c$ will be dynamically suppressed; hard gluon radiation at the subprocess vertex leads to asymptotic Sudakov form factor suppression of the color correlation effect.

Despite these general possibilities, it has now been shown that such color correlation effects actually cancel in QCD at least through two loop order, although it is present in individual diagrams. The cancellation through two loops was first demonstrated in perturbation theory by Lindsay, Ross, and Sachrajda [5] for scalar quark QCD interactions in both Feynman and light-cone gauge, and was subsequently confirmed in Feynman gauge by Bodwin *et al,* [4]. A detailed physical explanation of the two-loop cancellation is not known; it seems to be a consequence of both causality at high energies and local gauge invariance; neither by itself is sufficient. We also find that the cancellation breaks down at low energies or for long targets when condition, eq. (3), is not satisfied. It also fails in the case of spontaneous broken gauge theories with heavy gauge boson exchange because the trigluon graph is suppressed.

An example of the nature of the color correlation cancellations is shown in fig. 4 for $\pi\pi \to \ell\bar{\ell}X$. The diagrams shown are a gauge-invariant distinct class which have a non-trivial non-Abelian color factor and involve interactions with each of the incident spectators. The generality of the pion wave function precludes shifting of the transverse momentum interactions to other graphs. The various virtual two-gluon exchange amplitudes interfering with the zero gluon exchange amplitude each produces a $C_F C_A$ contribution which cancel in the sum. On the other hand, the imaginary part of the virtual graphs gives a non-zero contribution which potentially could lead to a color correlation at four loops. However, we find that even the potentially troublesome imaginary part is cancelled when one includes the

real emission diagrams of Figs. 6(d) and 6(e). Explicitly the sum of all the virtual and real emission amplitudes is proportional to

$$\left(C_F^2 - \frac{C_F C_A}{2}\right) \frac{2\vec{\ell}_{1\perp}\cdot\vec{\ell}_{1\perp}}{\ell_{1\perp}^2 \ell_{2\perp}^2} \frac{1}{\ell_1^+ + i\epsilon} \frac{1}{\ell_2^- + i\epsilon} \frac{1}{\ell_1^+\ell_2^- - (\vec{\ell}_{1\perp}+\vec{\ell}_{2\perp})^2 - i\mathcal{E}(-\ell_1^+)} \tag{9}$$

The integration over ℓ_2^- then leads to zero contributions for the leading power behavior. More generally, the proof of factorization of the Drell-Yan cross section can be divided into two distinct steps, as indicated in fig. 5. The first step is to prove that every contribution to initial state interactions in hadron-hadron scattering can be written as the convolution of two "eikonal-extended" structure functions as indicated in fig. 5(a). This is the "weak-factorization" ansatz proposed by Efremov and Radyushkin and by Collins, Soper, and Sterman [23] where each structure function has a eikonal factor attached which includes all of the elastic and inelastic initial state interactions of the corresponding incident annihilating quark or antiquark. Explicitly, the eikonal-extended structure function of the target system A is defined as [22]

$$\begin{aligned} P_{q/A}(x,k_\perp) = \frac{1}{2(2\pi)^3}\int dy^- \int d^2y_\perp\, e^{i(xP_A^+ y - \vec{k}_\perp\cdot\vec{y}_\perp)} \\ \times \langle A|\,\bar{\psi}_{DY}(0,y^-,\vec{y}_\perp)\gamma^+\psi_{DY}(0,0,\vec{0}_\perp)|A\rangle \end{aligned} \tag{10}$$

where

$$\Psi_{DY}(y^\nu) = P\exp -ig\int_{-\infty}^{0} d\lambda\, n\cdot A(y^\nu + \lambda n^\nu)\psi(y^\nu)$$

and n^μ is chosen such that $n\cdot\ell = 2\ell^3$ in the center-of-mass frame. The path-ordered exponential contains all of the interactions of the eikonal antiquark line with the color gauge field along the incident $\hat{z}$ direction up to the point of annihilation.

Recently, we have verified [13] that the weak factorization ansatz is correct through two loops in perturbation theory for $M(A+B\to\ell\bar{\ell}X)$ despite the complicated color-topological structure of the contributing diagrams. The proof relies on splitting each Feynman amplitude into separate structure functions using identities of the form

$$\frac{1}{A\ell^+ + i\epsilon}\frac{1}{-B\ell^- + i\epsilon} = \left(\frac{1}{A\ell^+ + i\epsilon}\frac{1}{B} + \frac{1}{-B\ell^- + i\epsilon}\frac{1}{A}\right)\frac{1}{\ell^+ - \ell^- + i\epsilon} \tag{11}$$

and then analytically continuing each contribution out of the Glauber regime to either large ℓ^- or large ℓ^+, corresponding to exchange gluons collinear with the beam or target, respectively. Finally, the use of collinear Ward identities allows one to organize gauge-related diagrams into the desired weak factorization form. We are continuing efforts to try to extend the proof beyond two loop order in QCD.

The second step required to prove factorization is to show that the structure function, eq. 10), is actually identical to the corresponding eikonal-extended structure function for deep inelastic-lepton-hadron scattering which includes a post-factor for the final state interactions of the struck quark [see fig. 5(b)]. This becomes intuitively obvious when one examines moments of the two structure functions. These moments differ only by terms proportional to powers of the integral $\int_{-\infty}^{0} dz\, E_z(z)$, where E_z is the longitudinal component of the chromo-electric field along the eikonal line. In the center of momentum frame the hadron has ultra-relativistic momentum along the z axis, and consequently the Lorentz-transformed longitudinal electric fields in the hadron are vanishing small. Thus all the moments, and therefore the structure functions themselves, become identical as $Q \to \infty$. Physically, the effective equality of the structure functions implies that the color fluctuations generated by initial and final interactions at high energies in massive lepton pair production and deep inelastic lepton scattering are basically equivalent [22].

At this point there is no convincing counterexample to standard QCD factorization for hadron-induced large momentum transfer reactions. Clearly if factorization is a general feature of gauge theories, then it is a novel and profound feature which demands explanation in fundamental terms [23]. In any event, the initial state interactions lead to new physical phenomena for the $Q_\perp$ distributions, e.g., the nuclear number dependence of $k_\perp$ fluctuations and associated particle production (see below). Furthermore, color correlations and breakdown of factorization do explicitly occur for power-law suppressed contributions which are sensitive to the length scale of the target. Such effects should be measureable for heavy nuclear targets at moderate Q^2.

Although our analysis is based on QCD perturbation theory our conclusions can be expressed in terms of rather general principles:

(1) Critical Momentum Scale. The characteristic momentum of each hard subprocess must be large compared to a scale set by the length of the target (or beam), as in eq. (3); otherwise the constituents, in passing through the target can lose a significant fraction of their longitudinal momentum to radiation, completely destroying any connection between the hadronic reaction and the distributions measured in deep inelastic scattering. This is related to the more general concept of the "formation zone".

(2) Formation Zone. The state of a hadronic system cannot be modified significantly in a time (in its rest system) less than its intrinsic scale [19]. Thus, a high energy quark cannot radiate a collinear gluon $q \to q + g$ inside of a target of length L if $s \gg \Delta(M^2)LM$ where $\Delta(M^2)$ is the change in the square of the invariant mass, and LM/s is proportional to the Lorentz-contracted length of the target in the quark rest frame. Similarly, the fragmentation of a quark into collinear hadrons (or vice versa) occurs *outside* of the target volume at high energies. We also note that interactions between quark or gluon constituents of the same hadron do not occur (to leading order in $1/s$) during the transit through the target volume. Thus high energy interactions of hadrons within nuclei are correctly described in terms of constituent quark and gluon propagation. The formation zone phenomena also implies that only a limited amount of energy is transferred to excitation processes in high energy heavy ion collisions.

(3) Large Longitudinal Range. The change of longitudinal momentum (in the CM) due to initial or final state interactions is so small that longitudinal structure in the target cannot be resolved in a target of length $L < \sqrt{s}/\langle \ell_\perp^2 \rangle$ (as measured in the CM frame).

(4) Color Singlet Cancellations. Large momentum transfer *exclusive* reactions are controlled by the Fock states with the minimum number of constituents at transverse distances $b_\perp^2 \sim (1/Q^2)$[24]. The initial and final state collisions can probe transverse distances no smaller than $1/\lambda$. Thus, such interactions cannot resolve the internal structure of the hadrons in exclusive reactions, and they do not couple to these color neutral objects. Formally, the initial and final state interactions cancel to leading order in $1/Q^2$ if one adds the contributions coming from all constituents of a color neutral hadron. This also implies that large momentum transfer quasi-elastic reactions such as $eA \to ep(A-1)$ and $\pi A \to \pi p(A-1)$ can

occur deep inside a nuclear target without multiple scattering or bremsstrahlung in the target [26]. Color singlet cancellations also eliminate initial and final state interactions of hadrons interacting directly in hard scattering inclusive reactions. For example, the "direct pion" [25] has no initial state interactions in $\pi_D g \to q\bar{q}$ (in $\pi p \to q\bar{q}X$), and no final state interactions in $(pp \to \pi X)$. There are thus no accompanying spectator hadrons accompanying along the meson in such processes. Similarly the higher twist $p_T^{-8} f(x_T, \theta_{cm})$ subprocess $\bar{p}_D\, q \to \bar{q}\,\bar{q}$ leads to the production of two jets at large p_T in $\bar{p}\,p \to \text{Jet} + \text{Jet} + X$ without beam spectators. We also note that the higher twist $F_L \sim 1/Q^2$ contribution to the meson structure function [27] is unaffected by initial and final state interactions. On the other hand, although they are power law suppressed at large momentum transfer, initial and final state interactions are expected to play an important role at moderate kinematic values, possibility leading to non-trivial helicity and interference effects [28]. Part of the difference between time-like and space-like form factors, e.g., $e^+e^- \to \pi^+\pi^-$ and $e^-\pi^+ \to e^-\pi^+$ is attributable to final state interactions, although the difference is suppressed by $\sim 1/Q^2$.

In contrast, virtually every large momentum transfer inclusive process in QCD is affected by initial and/or final state interactions. It is important to study the phenomenology of these interactions since they bear on the dynamics of quarks and gluons in hadronic matter and are evidentally related to the confinement mechanisms and the space-time "inside-outside" development of QCD jets [29]. Analysis of the role played by nuclear targets is clearly crucial in this study. Although the structure function measured in deep inelastic lepton scattering are unaffected by initial and final state interactions, the development of the final state jet distribution is modified by multiple scattering in the target. The transverse momentum of the struck quark relative to the current direction will obviously be broadened and multiplicity in the central region will be increased, thus affecting the fragmentation distribution of quarks into hadrons $D_{H/Q}(x, k_\perp)$. These effects should increase with the number of collisions in a nuclear target:

$$\delta\langle k_\perp^2\rangle = A^{1/3}\,, \quad \delta\langle n_{\text{central}}\rangle \propto A^{1/3}\,. \tag{12}$$

In addition, for long targets, energy-momentum conservation implies a correlated degradation of the leading particle distribution at large z. For low quark energies, collinear radiation can

be induced in the target and can drastically alter the longitudinal momentum fraction distributions.

The development of hadronic multiplicity in deep inelastic lepton scattering in the nucleus is particularly interesting since one is studying the influence of hadronic matter of quark jet propagation. As we have emphasized, formation of the leading particle in the jet occurs outside the nuclear volume at high energies. The inelastic final state interactions amount to cascading in the nucleus and demonstrate that, contrary to the usual assumptions made for the analysis of hadron-nucleus collisions, particle production in the target and central rapidity region cannot be correlated with the number of nucleons "wounded" by the beam. a model for the shape of the rapidity distribution based on "color cascading" is given in reference 30.

More generally any hard scattering inclusive process is accompanied by soft hadrons in the central rapidity region, which are the result of the initial state or final state interaction of the quark and gluon constituents. We emphasize that, even though the hard scattering cross section can be computed as if a single interactions occurs, the associated multiplicity reflects the full scope of the actual QCD dynamics.

In the case of hadron production at large transverse momentum in a nucleon or nuclear target collisions the inclusive cross section is increased by the $k_\perp$ smearing effects of the initial and final state interactions. the multiple scattering series in a nucleus [31] leads to terms roughly of order A^1, $A^{4/3}/p_\perp^2$, $A^{5/3}/p_\perp^4$, etc. The coefficient of the A^α terms with $\alpha > 1$ can be quite large, since one is smearing a cross section that falls very rapidly with $p_\perp$. Thus, strongly suppressed cross sections such as $pA \to \bar{p}X$ and $pA \to K^-X$ obtain a much larger nuclear enhancement from quark and gluon scattering effects than channels such as $pA \to \pi^+X$ or $pA \to K^+X$. In the case of direct γ production, the photon has no final state interactions, so only initial state interactions of the active q and g constituents are important. Similarly, at large x_T where direct subprocesses such as $gq \to \pi_D q$ or $qq \to \pi_D g$ are expected to dominate $pA \to \pi X$ production, only initial state interactions are important. Thus one can use direct photon reactions, photoproduction, Compton scattering, and direct hadron

interactions, especially the A-dependence of the cross sections, to eliminate and effectively isolate the effect of initial and final state interactions.

Nuclear initial and final state effects are, of course, enhanced in processes such as $A_1A_2 \to HX$. Nuclear targets also enhance the effects of multiple scattering processes that lead to multiple jets in the final state [32]. On the other hand, if the valence state of a hadron consists of constituents at small transverse separation, then the hadron can pass through the target with no color or hadronic interactions. An application of this idea to diffractive dissociation processes in nuclei is discussed in reference [33].

Processes such as $pp \to pp\mu\bar{\mu}$ [34], which occur via $\gamma\gamma \to \mu\bar{\mu}$ subprocesses, are also sensitive to the nature of initial state interactions. Unlike the corresponding lepton-induced reaction $ee \to ee\mu\bar{\mu}$, the initial state interactions of the two nucleons smear the transverse momentum distribution of the $\mu\bar{\mu}$ pair and can eliminate the strong peaking at $Q_\perp = 0$ associated with the γ poles. However, the cross section integrated over all $Q_\perp$ is unchanged.

3. Radiation null zones and other novel QCD effects [36]

A surprising feature of the subprocess cross section $\frac{d\sigma}{d\Omega}(u\bar{d} \to W^+\gamma)$, calculated in tree graph approximation in $SU(2) \times U(1)$ gauge theory, is the fact that each of the contributing tree graph helicity amplitudes vanishes near $\cos\theta^{\gamma d}_{CM} = 1/3$ (see fig. 6) [35]. In fact, this is a special case of a general theorem [36,37] for gauge theories applicable to any photon emission process: every tree-graph helicity amplitude $M^\mu_{\lambda_i \ldots \lambda_n}$ for radiation produced by the scattering of n incident and final particles vanishes at the kinematic domain such that all the ratios $Q_i/p_i \cdot k$ are equal:

$$\frac{Q_i}{p_i \cdot k} = \frac{Q_1}{p_1 \cdot k} \qquad i = 2, \ldots, n$$

(Because of charge and four-momentum conservation this is actually only $n-2$ independent conditions.) The Born cross section is thus identically zero in this kinematic domain, which we will refer to as the "null zone". Notice that the photon energy is essentially unrestricted, not limited to the usual infrared regime of soft photon theorems. The general proof of this result for gauge theories for processes with any number of charged spin 0, $\frac{1}{2}$ or 1 particles

with minimal electromagnetic coupling is given in reference 36. The essential elements of the proof are:

(1) In the null zone the radiation from the classical (convection) currents of the external lines destructively interfere.

(2) The spin currents of charged spin $\frac{1}{2}$ and spin 1 particles in gauge theory tree graph amplitudes can be represented in the form of an infinitesimal psuedo–Lorentz transformation since in each case $g = 2$. In the null zone the radiation due to the spin currents then cancel, because of Lorentz invariance. The cancellation of spin current contributions is also related to the fact that for any spin $g = 2$ implies that the spin precession and Larmor frequencies are identical [38]. The radiation associated with derivative couplings and seagull contributions also cancel, again because they can be related to infinitesimal Lorentz transformations.

(3) The radiation from internal lines can be rewritten using Ward-type identities in the form of a sum of external line emission processes, each of which again give vanishing contribution in the null zone.

The null zone cancellations only hold for tree graph amplitudes — quantum corrections due to diagrams with internal loops lead to $g \neq 2$ and break the exact destructive interference [39]. The null zone phenomena, being a general result of local gauge theory, is interesting from several points of view:

(a) In the case of $u\bar{d} \to W^+\gamma$, verification of a dip in the cross section at the null zone point $\cos\theta^{\gamma d}_{cm} = \frac{1}{\beta_q}\,(Q_u - Q_{\bar{d}})/Q_W = \frac{1}{3} + O(m_q^2/m_W^2)$ tests not only that the gyromagnetic ratios g_W and g_q have the Dirac value $g = 2$ in gauge theories, but it also measures the fractional charge of the quark. The corrections from QCD higher order loop diagrams are $O(\alpha_s(m_W^2))$. In addition there are k_T-smearing and off-shell corrections due to quark transverse momentum of order $\langle k_\perp^2 \rangle / m_W^2$.

(b) We have emphasized that the null zone cancellation is a general property for all scattering amplitudes involving photon emission calculated from tree graphs in gauge theory. Most often the null zone region lies outside the physical kinematic regime unless the conditions described in references [36,40] are met; for example: all the incident and final charged particles have to have the same sign of charge such as $u\bar{d} \to u\bar{d}\gamma$ [36]. Other measurable

examples include the QED process $d\sigma(e^-e^- \to e^-e^-\gamma)$ which vanishes to leading order in α in the two-dimensional region illustrated in fig. 7. Another interesting process is $e^+e^+ \to Q\bar{Q}\gamma$; as shown by Passarino [40], the null zone for this process can be used to measure the heavy quark mass.

(c) Independent of whether the null zone for a given process lies in the physical region, any tree graph radiation gauge theory amplitude can be written in the compact representation [36,37]

$$M^\mu = \sum_{i-2}^{n-1} \left(\frac{Q_i}{p_i \cdot k} - \frac{Q_1}{p_1 \cdot k} \right) \hat{M}_i^\mu$$

independent of helicity.

(d) The vanishing of the cross section at a specific point in momentum space is consistent with the uncertainty principle since the null zone condition only depends on the external lines which have unspecified position. The results are also consistent with the correspondence principle: the classical ($\hbar = 0$) tree graph limit of gauge theories is consistent with classical radiation. These results imply that the only consistent possiblity for electromagnetic spin couplings at the tree graph level is $g = 2$ for any spin; $g \neq 2$ must come from quantum corrections. This conclusion is also consistent with the Drell-Hearn Gerasimov sum rule. Conversely, effective local field theories of nucleon and mesons which have $g_N \neq 2$ at the tree graph level are inconsistent with the correspondence principle. The null zone phenomena thus provide another criteria for constructing acceptable fundamental theories.

In the remainder of the section we will briefly review several other novel QCD effects; further details may be found in the referenced papers.

Higher Twist Anomalies.

As described in reference 3, there are now a large number of higher twist photon and direct hadron subprocesses which can be absolutely normalized using the analysis of reference 41. In particular, the longitudinal structure function of the pion can be absolutely normalized in terms of the pion form factor [42].

$$F_{2\pi}(x, Q^2) = A(1-x)^2 + \frac{C}{Q^2} x^2$$

where

$$C = \sum e_q^2 \frac{C_F}{2\pi} \int_{\mu^2/(1-x)}^{Q^2/x} d\ell^2 \alpha_s(\ell^2) F_\pi(\ell^2) \simeq 0.1\ GeV^2 .$$

This basic QCD prediction can be tested for the dominance of $(C/Q^2)\sin^2\theta$ dependence of the Drell-Yan $\pi p \to \ell\bar{\ell}X^-$ cross section at $x_1 \sim 1$. In addition one expects contributions of order $(C/Q)(1-x_a)\sin 2\theta\cos\phi$ (θ and ϕ are the angles of the ℓ_+ in the γ^* rest frame) from longitudinal-scalar interference; as emphasized by Pire and Ralston [43], these phase-sensitive contributions can have an interesting interference pattern due to Sudakov form factor effects.

The higher twist contributions to the nucleon structure function at $x \sim 1$ have now been systematically computed to lowest order in α_s by Blankenbecler, Gunion, and Nason [44]. The result computed from the set of two-gluon exchange diagrams has the form

$$F_{2N}(x,Q^2) = A(1-x)^3 + \frac{B(1-x)}{Q^2} + \frac{C}{Q^2}\ (1-x)^2$$

where $B \simeq -6\mu^2$, and $C \simeq 800\ \mu^2$. Here μ^2 is a typical hadronic scale, estimated as $\mu^2 = 0.01\ GeV$. The astonishingly large size of the $C(1-x)^2/Q^2$ term implies large power-law contributions to the scale-breaking of deep inelastic lepton-nucleon structure functions, consistent with those parametrized by Abbott et al [45].

Intrinsic Charm.

The dynamical origin of heavy quark states in hadron collisions such as charm production is still not satisfactorily understood. The data [46] suggests large contributions of a diffractive nature leading to fast forward charm production $pp \to \Lambda_c X$ at large x_L at ISR energies; the nuclear A-dependence of the charm production cross section at large x_L appears similar to that of total cross sections. It has been suggested [47] that the magnitude and forward behavior of the charm production cross section at high energies can be understood if the wave function of the proton contains charmed quarks at the 1% probability level with a valence-like $G_{c/p} \sim (1-x)^3$ behavior ("intrinsic" charm) in contrast to the soft dependence $\sim (1-x)^7$ usually associated with sea quarks, $g \to c\bar{c}$, or QCD evolution.

One can motivate the valence-like distribution of heavy virtual quarks in a light hadron using an atomic physics analogy: Consider the $\mu^+\mu^-e^+e^-$ contribution to the positronium Fock state wavefunction generated by $\mu^+\mu^-$ vacuum polarization, the same twist–six contributions

which yield the Serber-Uehling potential. The μ^+ and μ^- are produced dominantly at low velocities since this minimizes the off-shell energy of the virtual state. If one now views the atom from a moving relativistic frame, then the fact that the leptons all have nearly the same velocity implies that the muons carry a large momentum fraction since momentum increases with mass. Similarly, a Fock state of an ordinary hadrons containing heavy quarks will be dominated by configurations in which heavy quarks have low velocity relative to the valence quarks, since this increases the QCD binding as well as decreases the off-shell energy. Again this implies that the intrinsic heavy quark components associated with the hadron wavefunction are produced dominantly at large x. If the atomic physics analogy is correct, then the probability for such Fock states scales as $1/m_Q^2$ and is controlled by $\alpha_s(\mu^2)$ where μ is the ordinary hadronic scale. The diffractive excitation of such states at very high energies (where $t_{\rm min}$ effects are negligible) then leads to large diffractive cross sections proportional to $1/m_Q^2$ with A^α ($\alpha < 1$) dependence. A complete understanding of the charm production cross section requires an understanding of both central region $gg \to c\bar{c}$ (with A^1 dependence) and the diffractive intrinsic heavy quark components. Of course, one of the most important applications are the implications for top quark production in high energy hadronic collisions using the

diffractive trigger. The predicted cross section is $\sigma_{t\bar{t}} \sim \sigma_{c\bar{c}}\, m_c^2/m_t^2$ modulo a phase-space suppression $\sim (1 - s_{th}/s)^n$. Similarly, one also expects diffractive production of supersymmetric colored particles such as squarks and gluinos in supersymetric QCD. In general any particle/antiparticle system which couples through color SU(3) interactions is present in the Fock state structure of ordinary hadrons and can be diffractively excited in high energy collisions.

4. Nuclear chromodynamics: applications of QCD to nuclear systems [8]

4.1 Introduction to NCD

In QCD, the fundamental degrees of freedom of nuclei as well as hadrons are postulated to be the spin-1/2 quark and spin-1 gluon quanta. Nuclear systems are identified as color-singlet composites of quark and gluon fields, beginning with the six-quark Fock component of the deuteron. An immediate consequence is that nuclear states are a mixture of several color

representations which *cannot* be described solely in terms of the conventional nucleon, meson, and isobar degrees of freedom: there must also exist "hidden color" multiquark wavefunction components—nuclear states which are not separable at large distances into the usual color singlet nucleon clusters. There are a number of immediate consequences for nuclear dynamics:

1. The electromagnetic and weak currents within a nucleus are carried solely by the quark fields at any momentum transfer scale $Q^2 = -q_\mu^2$. In the deep inelastic, large momentum and energy transfer domain, the lepton scatters essentially incoherently off of the individual quark constituents of the nucleus, giving point-like cross sections characteristics of Bjorken scaling,modified by logarithmic corrections to scale-invariance due to QCD radiative corrections. At low momentum transfer the quark currents become coherent, giving cross sections characteristics of multiquark, nucleonic, or mesonic currents.

2. The nuclear force between nucleons can in principle be represented at a fundamental level in QCD in terms of quark interchange (equivalent at large distances to pion and other meson exchange) and multiple-gluon exchange [9]. Although calculations from first principles are still too complicated, recent results derived from effective potential, bag, and soliton models [48] suggests that many of the basic features of the nuclear force can be understood from the underlying QCD substructure. At a more basic level one can give a direct proof [49] from perturbative QCD that the nucleon-nucleon force must be repulsive at short distances.

3. Because of asymptotic freedom, the effective strength of QCD interactions becomes logarithmically weak at short distances and large momentum transfer

$$\alpha_s(Q^2) = \frac{4\pi}{\beta_0 \log(Q^2/\Lambda^2_{\rm QCD})} \qquad (Q^2 \gg \Lambda^2)\,. \tag{13}$$

[Here $\beta_0 = 11 - \frac{2}{3}\,n_f$ is derived from the gluonic and quark loop corrections to the effective coupling constant; n_f is the number of quark contributions to the vacuum polarizations with $m_F^2 \lesssim Q^2$.] The parameter $\Lambda_{\rm QCD}$ normalizes the value of $\alpha_s(Q_0^2)$ at a given momentum transfer $Q_0^2 \gg \Lambda^2$, given a specific renormalization or cutoff scheme. Recently α_s has been determined fairly unambiguously using the measured

branching ratio for upsilon radiative decay $\Upsilon(b\bar{b}) \to \gamma X$: [50,51]

$$\alpha_s(0.157\ M_\Upsilon) = \alpha_s(1.5\ GeV) = 0.23 \pm 0.13\ . \tag{14}$$

Taking the standard $\overline{MS}$ dimensional regularization scheme, this gives $\Lambda_{\overline{MS}} = 119 \begin{smallmatrix} + 52 \\ - 34 \end{smallmatrix}$ MeV. In more physical terms, the effective potential between infinitely heavy quarks has the form [$C_F = 4/3$ for $n_c = 3$] (see Appendix).

$$V(Q^2) = -C_F\ \frac{4\pi\alpha_V(Q^2)}{Q^2}$$
$$\alpha_V(Q^2) = \frac{4\pi}{\beta_0 \log(Q^2/\Lambda_V^2)} \qquad (Q^2 \gg \Lambda_V^2) \tag{15}$$

where [51] $\Lambda_V = \Lambda_{\overline{MS}}\, e^{5/6} \simeq 270 \pm 100\ MeV$. Thus the effective physical scale of QCD is $\sim 1\ f_m^{-1}$. At momentum transfers beyond this scale, α_s becomes small, QCD perturbation theory becomes applicable, and a microscopic description of short-distance hadronic and nuclear phenomena in terms of quark and gluon subprocesses becomes viable. In this lecture we will particularly emphasize the use of asymptotic freedom and light-cone quantization to derive factorization theorems [50-53], rigorous boundary conditions, and exact results for nuclear amplitudes at short distances [49,54,55]. This includes the nucleon form factor at large momentum transfer [53], meson photoproduction amplitudes, deuteron photo- and electro-disintegration [55] and most important for nuclear physics, exact results for the form of the form factor of nuclei at large momentum transfer [49,54]. Eventually it should be possible to construct fully analytic nuclear amplitudes which at low energies fit the standard chiral constraints and low energy theories of traditional nuclear physics while at the same time satisfying the scaling laws and anomalous dimension structure predicted by QCD at high momentum transfer.

4. Since QCD has the same natural length scale $\sim 1\ fm$ as nuclear physics it is difficult to argue that nuclear physics can be studied in isolation from QCD. Thus one of the most interesting questions in nuclear physics is the transition between conventional meson-nucleon degrees of freedom to the quark and gluon degrees of freedom of QCD. As one probes distances shorter than $\Lambda_{\rm QCD}^{-1} \sim 1\ fm$ the meson-nucleon degrees of freedom must break down, and we expect new nuclear phenomena, new physics intrinsic to

composite nucleons and mesons, and new phenomena outside the range of traditional nuclear physics. One apparent signal for this is the experimental evidence [10] from deep inelastic lepton-nucleus scattering that nuclear structure functions deviate significantly from simple nucleon additivity, much more than would have been expected for lightly bound systems. Further, as discussed in section 4.5, there are many areas where QCD predictions conflict with traditional concepts of nuclear dynamics.

4.2 Exclusive nuclear processes

One area of important progress in hadron physics in the past few years has been the extension of QCD predictions to the domain of large momentum transfer hadronic and nuclear amplitudes including nuclear form factors, deuteron photodisintegration, etc. [7]. A key result is that such amplitudes factorize at large momentum transfer in the form of a convolution of a hard scattering amplitude T_H which can be computed perturbatively from quark-gluon subprocesses multiplied by process-independent "distribution amplitudes" $\phi(x,Q)$ which contain all of the bound-state non-perturbative dynamics of each of the interacting hadrons. To leading order in $1/Q$ the scattering amplitude has the form [see fig. 8(a)]

$$\mathcal{M} = \int_0^1 T_H(x_j,Q) \prod_{H_i} \phi_{H_i}(x_j,Q)[dx_j] \; . \tag{16}$$

Here T_H is the probability amplitude to scatter quarks with fractional momentum $0 < x_j < 1$ from the incident to final hadronic directions, and ϕ_{H_i} is the probability amplitude to find quarks in the wavefunction of hadronic H_i collinear up to the scale Q, and

$$[dx_j] = \prod_{j=1}^{n_i} dx_j \delta\Big(1 - \sum_k^{n_i} x_k\Big) \tag{17}$$

A key to the derivation of this factorization of perturbative and non-perturbative dynamics is the use of a Fock basis $\{\psi_n(x_i, \vec{k}_{\perp i}, \lambda_i)\}$ defined at equal $\tau = t + z/c$ on the light-cone to represent relativistic color singlet bound states [52]. Here λ_i is the helicity; $x_i \equiv (k^0 + k^z)/(p^0 + p^z)$, $(\sum_{i=1}^n x_i = 1)$, and $\vec{k}_{\perp i}$, $(\sum_{i=1}^n \vec{k}_{\perp i} = 0)$ are the relative momentum coordinates. Thus the proton is represented as a column vector of states ψ_{qqq}, ψ_{qqqg}, $\psi_{qqq\bar{q}q}$ .... In the light-cone gauge, $A^+ = A^0 + A^3 = 0$, only the minimal "valence" Fock state needs to be considered at large momentum transfer since any additional quark or gluon forced to

absorb large momentum transfer yields a power-law suppressed contribution to the hadronic amplitude. For example at large Q^2, the baryon form factor takes the form [53] [fig. 8(a)]

$$F_B(Q^2) = \int_0^1 [dy] \int_0^1 [dx]\ \phi_B^\dagger(y_j, Q) T_H(x_i, y_j, Q) \phi_B(x_i, Q) \ , \tag{18}$$

where to leading order in $\alpha_s(Q^2)$, T_H is computed from $3q + \gamma^* \to 3q$ tree graph amplitudes: [fig. 8(b)]

$$T_H = \left[\frac{\alpha_s(Q^2)}{Q^2}\right]^2 f(x_i, y_j) \tag{19}$$

and

$$\phi_B(x_i, Q) = \int [d^2 k_\perp]\ \psi_V(x_i, \vec{k}_\perp) \theta(k_\perp^2 < Q^2) \tag{20}$$

is the valence three-quark wavefunction evaluated at quark impact separation $b_\perp \sim O(Q^{-1})$. Since ϕ_B only depends logarithmically on Q^2 in QCD, the main dynamical dependence of $F_B(Q^2)$ is the power behavior $(Q^2)^{-2}$ derived from scaling of the the elementary propagators in T_H. Thus, modulo logarithmic factors, one obtains a dimensional counting rule for any hadronic or nuclear form factor at large Q^2 ($\lambda = \lambda' = 0$ or $1/2$) [56]

$$F(Q^2) \sim \left(\frac{1}{Q^2}\right)^{n-1} , \tag{21}$$

$$F_1^N \sim \frac{1}{Q^4} , \quad F_\pi \sim \frac{1}{Q^2} , \quad F_d \sim \frac{1}{Q^{10}} , \tag{22}$$

where n is the minimum number of fields in the hadron. Since quark helicity is conserved in T_H and $\phi(x_i, Q)$ is the $L_z = 0$ projection of the wavefunction, total hadronic helicity is conserved [57] at large momentum transfer for any QCD exclusive reaction. The dominant nucleon form factor thus corresponds to $F_1(Q^2)$ or $G_M(Q^2)$; the Pauli form factor is suppressed by an extra power of Q^2. In the case of the deuteron, the dominant form factor has helicity $\lambda = \lambda' = 0$, corresponding to $\sqrt{A(Q^2)}$. The general form of the logarithmic dependence of $F(Q^2)$ can be derived from the operator product expansion at short distance or by solving an evolution equation for the distribution amplitude computed from gluon exchange [fig. 8(c)],

as we discuss for the deuteron. The result for the large Q^2 behavior of the baryon form factor in QCD is [7]

$$F_B(Q^2) = \frac{\alpha_s^2(Q^2)}{Q^4} \sum_{n,m} d_{nm} \left(ln \ \frac{Q^2}{\Lambda^2} \right)^{-\gamma_m - \gamma_n} \tag{23}$$

where the γ_n are computable anomalous dimensions of the baryon three-quark wave function at short distance and the d_{mn} are determined from the value of the distribution amplitude $\phi_B(x, Q_0^2)$ at a given point Q_0^2. Asymptotically the dominant term has the minimum anomalous dimension. The predicted sign of $G_M^p(Q^2)$ at large Q^2 is the same as $G_M^p(0)$. The dominant part of the form factor comes from the region of the x integration where each quark has a finite fraction of the light cone momentum; the end point region where the struck quark has $x \simeq 1$ and spectator quarks have $x \sim 0$ is asymptotically suppressed by quark (Sudakov) form factor gluon radiative corrections.

As shown in fig. 9 the power laws (21, 22) predicted by perturbative QCD are consistent with experiment [58]. The behavior $Q^4 G_M(Q^2) \sim$ *const* at large Q^2 provides a direct check that the minimal Fock state in the nucleon contains three quarks and that the quark propagator and the $qq \to qq$ scattering amplitudes are approximately scale-free. More generally, the nominal power law predicted for large momentum transfer exclusive reactions is given by the dimensional counting rule $\mathcal{M} \sim Q^{4-n_{TOT}} F(\theta_{cm})$ where n_{TOT} is the total number of elementary fields which scatter in the reaction. The predictions are apparently compatible with experiment. In addition, for some scattering reactions there are contributions from multiple scattering diagrams (Landshoff contributions) which together with Sudakov effects can lead to small power-law corrections, as well as a complicated spin, and amplitude phase phenomenology. Recent measurements [59] of $\gamma\gamma \to \pi^+\pi^-$, K^+K^- at large invariant pair mass appear to confirm the QCD predictions [60].

In principle it should be possible to use measurements of the scaling and angular dependence of the $\gamma\gamma \to M\bar{M}$ reactions to measure the shape of the distribution amplitude $\phi_M(x, Q)$. An actual calculation of $\phi(x, Q)$ from QCD requires non-perturbative methods such as lattice gauge theory, or more directly, the solution of the light-cone equation of motion

$$\left[M^2 - \sum_{i=1}^{n} \left(\frac{k_\perp^2 + m^2}{x} \right)_i \right] \Psi = V_{\rm QCD} \Psi \tag{24}$$

The explicit form for the matrix representation of $V_{\rm QCD}$ and a discussion of the infrared and ultraviolet regulation required to interpret (24) is given in reference 52. Thus far experiments has not been sufficiently precise to measure the logarithmic variation from dimensional counting rules predicted by QCD. Checks of the normalization of $(Q^2)^{n-1}F(Q^2)$ require independent determinations of the valence wavefunction. The relatively large normalization of $Q^4G_M^p(Q^2)$ at large Q^2 can be understood if the valence three-quark state has small transverse size, i.e., is large at the origin [52,61]. The physical radius of the proton measured from $F_1(Q^2)$ at low momentum transfer then reflects the contributions of the higher Fock states $qqqg$, $qqq\bar{q}q$ (or meson cloud), etc. A small size for the proton valence wavefunction (e.g., $R^p_{qqq} \sim 0.3\ fm$) can also explain the large magnitude of $\langle k_\perp^2 \rangle$ of the intrinsic quark momentum distribution needed to understand in hard-scattering inclusive reactions. The necessity for small valence state Fock components can be demonstrated explicitly for the pion wavefunction, since $\psi_{q\bar{q}}/\pi$ is constrained by sum rules derived from $\pi^+ \to \ell^+\nu$, and $\pi^- \to \gamma\gamma$. One finds a valence state radius $R^\pi_{q\bar{q}} \sim 0.2\,fm$, corresponding to a probability $P^\pi_{q\bar{q}} \sim 1/4$. A detailed discussion is given in reference 61.

4.3 The deuteron in QCD

Of the five color-singlet representations of six quarks, only one corresponds to the usual system of two color singlet baryonic clusters. (Explicit representations are given in reference 62). Note that the exchange of a virtual gluon in the deuteron at short distance inevitably produces Fock state components where the three-quark clusters correspond to color octet nucleons or isobars. Thus, in general, the deuteron wavefunction will have a complete spectrum of hidden-color wavefunction components, although it is likely that these states are important only at small internucleon separation [63].

Despite the complexity of the multi-color representations of nuclear wavefunctions, the analysis [49] of the deuteron form factor at large momentum transfer can be carried out in parallel with the nucleon case. Only the minimal six-quark Fock state needs to be considered

to leading order in $1/Q^2$. The deuteron form factor can then be written as a convolution (see fig. 10),

$$F_d(Q^2) = \int_0^1 [dx]\ [dy]\ \phi_d^\dagger(y,Q)\ T_H^{6q+\gamma^*\to 6q}(x,y,Q)\ \ \phi_d(x,Q)\ , \tag{25}$$

where the hard scattering amplitude scales as

$$T_H^{6q+\gamma^*\to 6q} = \left[\frac{\alpha_s(Q^2)}{Q^2}\right]^5 t(x,y)\ \ [1+O(\alpha_s(Q^2))] \tag{26}$$

The anomalous dimensions γ_n^d are calculated from the evolution equations for $\phi_d(x_i,Q)$ derived to leading order in QED from pairwise gluon-exchange interactions: ($C_F = 4/3$, $C_d = -C_F/5$)

$$\prod_{k=1}^{6} x_k \left[\frac{\partial}{\partial\xi} + \frac{3C_F}{\beta}\right]\tilde{\Phi}(x_i,Q) = -\frac{C_d}{\beta}\int_0^1 [dy]\ V(x_i,y_i)\,\tilde{\Phi}(y_i,Q)\ . \tag{27}$$

Here we have defined

$$\Phi(x_i,Q) = \prod_{k=1}^{6} x_k\,\tilde{\Phi}(x_i,Q), \tag{28}$$

and the evolution is in the variable

$$\xi(Q^2) = \frac{\beta_0}{4\pi}\int_{Q_0^2}^{Q^2}\frac{dk^2}{k^2}\alpha_s(k^2) \sim ln\left(\frac{ln\frac{Q^2}{\Lambda^2}}{ln\frac{Q_o^2}{\Lambda^2}}\right)\ . \tag{29}$$

The kernel V is computed to leading order in $\alpha_s(Q^2)$ from the sum of gluon interactions between quark pairs. The general matrix representations of γ_n with bases $\prod_{i=1}^5 x_i^{m_i} >$ are given in reference 62. The leading anomalous dimension γ_0, corresponding to the eigenfunction $\tilde{\Phi}(x_i) = 1$, is $\gamma_0 = (6/5)(C_F/\beta_0)$.

In order to make more detailed and experimentally accessible predictions, we will define the "reduced" nuclear form factor [54,55] in order to remove the effects of nucleon compositeness:

$$f_d(Q^2) \equiv \frac{F_d(Q^2)}{F_N^2(Q^2/4)}\ . \tag{30}$$

The arguments for the nucleon form factors (F_N) are $Q^2/4$ since in the limit of zero binding energy each nucleon must change its momentum from $\sim p/2$ to $(p+q)/2$. Since the leading

anomalous dimensions of the nucleon distribution amplitude is $C_F/2\beta$, the QCD prediction for the asymptotic Q^2-behavior of $f_d(Q^2)$ is [49]

$$f_d(Q^2) \sim \frac{\alpha_s(Q^2)}{Q^2}\left(ln\frac{Q^2}{\Lambda^2}\right)^{-\frac{2}{5}\frac{C_F}{\beta}} , \tag{31}$$

where $-(2/5)(C_F/\beta) = -8/145$ for $n_f = 2$.

Although this QCD prediction is for asymptotic momentum transfer, it is interesting to compare (32) directly with the available high Q^2 data [58] (see fig. 11). In general one would expect corrections from higher twist effects (e.g., mass and $k_\perp$ smearing), higher order contributions in $\alpha_s(Q^2)$, as well as non-leading anomalous dimensions. However, the agreement of the data with simple $Q^2 f_d(Q^2) \sim const$ behavior for $Q^2 > 1/2$ GeV^2 implies that, unless there is a fortuitous cancellation, all of the scale-breaking effects are small, and the present QCD perturbative calculations are viable and applicable even in the nuclear physics domain. The lack of deviation from the QCD parameterization also suggests that the parameter Λ in (32) is small. A comparison with a standard definition such as $\Lambda_{\overline{MS}}$ would require a calculation of next to leading effects. A more definitive check of QCD can be made by calculating the normalization of $f_d(Q^2)$ from T_H and the evolution of the deuteron wave function to short distances. It is also important to confirm experimentally that the helicity $\lambda = \lambda' = 0$ form factor is indeed dominant.

The calculation of the normalization $T_H^{6q+\gamma^* \to 6q}$ to leading order in $\alpha_s(Q^2)$ will require the evaluation of $\sim$ 300,000 Feynman diagrams involving five exchanged gluons. Fortunately this appears possible using the algebraic computer methods introduced in reference 64. The method of setting the appropriate scale $\hat{Q}$ of $\alpha_s^5(\hat{Q}^2)$ in T_H is given in reference 51.

We note that the deuteron wave function which contributes to the asymptotic limit of the form factor is the totally antisymmetric wave function corresponding to the orbital Young symmetry given by [[6]] and isospin (T) + spin (S) Young symmetry given by {33}.
The deuteron state with this symmetry is related to the NN, $\Delta\Delta$, and hidden color (CC) physical bases, for both the $(TS) = (01)$ and (10) cases, by the formula [65]

$$\psi_{[[6]]\{33\}} = \sqrt{\frac{1}{9}}\ \psi_{NN} + \sqrt{\frac{4}{45}}\ \psi_{\Delta\Delta} + \sqrt{\frac{4}{5}}\ \psi_{CC}\ . \tag{32}$$

Thus the physical deuteron state, which is mostly ψ_{NN} at large distance, must evolve to the $\psi_{[[6]]\{33\}}$ state when the six quark transverse separations $\vec{b}^i_\perp \leq O(1/Q) \to 0$. Since this state is 80% hidden color, the deuteron wave function cannot be described by the meson-nucleon isobar degrees of freedom in this domain. The fact that the six-quark color singlet state inevitably evolves in QCD to a dominantly hidden-color configuration at small transverse separation also has implications for the form of the nucleon-nucleon ($S_z = 0$) potential, which can be considered as one interaction component in a coupled channel system. As the two nucleons approach each other, the system must do work in order to change the six-quark state to a dominantly hidden color configuration; i.e., QCD requires that the nucleon-nucleon potential must be repulsive at short distances [47,49] (see fig. 12).

The evolution equation for the six-quark system suggests that the distance where this change occurs is in the domain where $\alpha_s(Q^2)$ most strongly varies. The general solutions of the evolution equation for multiquark systems will be given in reference [66.1]. Some of the solutions are orthogonal to the usual nuclear configurations which correspond to separated nucleons or isobars at large distances. Such solutions could be connected with the anomalous phenomena observed in heavy ion collisions.

4.4 Reduced nuclear amplitudes [55]

One of the basic problems in the analysis of nuclear scattering amplitudes is how to consistently account for the effects of the underlying quark/gluon component structure of nucleons. Traditional methods based on the use of an effective nucleon/meson local Lagrangian field theory are not really applicable (see section 4.5), giving the wrong dynamical dependence in virtually every kinematic variable for composite hadrons. The inclusion of *ad hoc* vertex form factors is unsatisfactory since one must understand the off-shell dependence in each leg while retaining gauge invariance; such methods have little predictive power. On the other hand, the explicit evaluation of the multiquark hard-scattering amplitudes needed to predict the normalization and angular dependence for a nuclear process, even at leading order in α_s requires the consideration of millions of Feynman diagrams. Beyond leading order one must include

contributions of non-valence Fock states wavefunctions, and a rapidly expanding number of radiative corrections and loop diagrams.

The reduced amplitude method [54,55], although not an exact replacement for a full QCD calculation, provides a simple method for identifying the dynamical effects of nuclear substructure, consistent with covariance, QCD scaling laws and gauge invariance. The basic idea has already been introduced for the reduced deuteron form factor. More generally if we neglect nuclear binding, then the light-cone nuclear wavefunction can be written as a cluster decomposition of collinear nucleons: $\psi_{q/A} = \psi_{N/A} \prod_N \Psi_{q/N}$ where each nucleon has 1/A of the nuclear momentum. A large momentum transfer nucleon amplitude then contains as a factor the probability amplitude for each nucleon to remain intact after absorbing 1/A of the respective nuclear momentum transfer $\sqrt{-t}/A$. We can identify each probability amplitude with the respective nucleon form factor $F\left(\hat{t}_i = \frac{1}{A^2}\ t_A\right)$. Thus for any exclusive nuclear scattering process, we define the reduced nuclear amplitude

$$m = \frac{\mathcal{M}}{\prod_{i=1}^{A} F_N(\hat{t}_i)} \tag{33}$$

The QCD scaling law for the reduced nuclear amplitude m is then identical to that of nuclei with point-like nuclear components: e.g., the reduced nuclear form factors obey

$$f_A(Q^2) \equiv \frac{F_A(Q^2)}{\left[F_N(Q^2/A^2)\right]^A} \sim \left[\frac{1}{Q^2}\right]^{A-1}. \tag{34}$$

Comparisons with experiment and predictions for leading logarithmic corrections to this result are given in references [19,55] In the case of photo- (or electro-) disintegration of the deuteron one has

$$m_{\gamma d \to np} = \frac{\mathcal{M}_{\gamma d \to np}}{F_n(t_n) F_p(t_p)} \sim \frac{1}{p_T}\ f(\theta_{cm}) \tag{35}$$

i.e., the same elementary scaling behavior as for $\mathcal{M}_{\gamma M \to q\bar{q}}$. Comparison with experiment [66] is encouraging (see fig. 13), showing that as was the case for $Q^2 f_d(Q^2)$, the perturbative QCD scaling regime begins at $Q^2 \geq 1\ GeV^2$. Detailed comparisons and a model for the angular dependence and the virtual photon-mass dependence of deuteron electrodisintegration are discussed in reference 55. Other potentially useful checks of QCD scaling of reduced

amplitudes are

$$m_{pp\to d\pi+} \sim p_T^{-2}\, f(t/s)$$

$$m_{pd\to H^3\pi+} \sim p_T^{-4}\, f(t/s) \qquad (36)$$

$$m_{\pi d\to \pi d} \sim p_T^{-4}\, f(t/s)\,.$$

It is also possible to use these QCD scaling laws for the reduced amplitude as a parametrization for the background for detecting possible new dibaryon resonance states.

4.5 Limitations of traditional nuclear physics [67]

The fact that the QCD prediction for the reduced form factor $Q^2 f_d(Q^2) \sim const$ appears to be an excellent agreement with experiment for $Q^2 > 1\ GeV^2$ provides an excellent check on the six-quark description of the deuteron at short-distance as well as the scale-invariance of the $qq \to qq$ scattering amplitude. It should also be emphasized that the impulse approximation form used in standard nucleon physics calculations

$$F_d(Q^2) = F_N(Q^2) \times F_{\text{Body}}(Q^2) \qquad (37)$$

is invalid in QCD at large Q^2 since off-shell nucleon form factors enter [see fig. 7(a)]. The region of validity [68] of (37) is restricted to $Q^2 < \lambda_H^2$ where λ_H^2 is a hadronic scale. The traditional treatment of nuclear form factors also overestimates the contribution of meson exchange currents [fig. 14(b)] and $N\bar{N}$ contributions [fig. 14(c)] since they are strongly suppressed by vertex form factors as we shall show in this section.

At long distances and low, non-relativistic momenta, the traditional description of nuclear forces and nuclear dynamics based on nucleon, isobar, and meson degrees of freedom appears to give a viable phenomenology of nuclear reactions and spectroscopy. It is natural to try to extend the predictions of these models to the relativistic domain, e.g., by utilizing local meson-nucleon field theories to represent the basic nuclear dynamics, and to use an effective Dirac equation to describe the propagation of nucleons in nuclear matter [66]. An interesting question is whether such approaches can be derived as a "correspondence" limit of QCD, at least in the low momentum transfer ($Q^2 R_p^2 \ll 1$) and low excitation energy domain ($Mv \ll M'^2 - M^2$).

The existence of hidden-color Fock state components in the nuclear state precludes an exact treatment of nuclear properties based on meson-nucleon-isobar degrees of freedom since these hadronic degrees of freedom do not form a complete basis on QCD. Since the deuteron form factor is dominated by hidden color states at large momentum transfer, it cannot be described by np, $\Delta\Delta$ wavefunction components on meson exchange currents alone. It is likely that the hidden color states give less than a few percent correction to the global properties of nuclei; nevertheless, since extra degrees of freedom lower the energy of a system it is even conceivable that the deuteron would be unbound were it not for its hidden color components!

Independent of hidden color effects, we can still ask whether is it possible—in principle—to represent composite systems such as meson and baryons as local fields in a Lagrangian field theory, at least for sufficiently long wavelengths such that internal structure of the hadrons cannot be discerned. Here we will outline a method to construct an effective Lagrangian of this sort. First, consider the ultraviolet-regulated QCD Lagrangian density $\mathcal{L}^{\kappa}_{\rm QCD}$ defined such that all internal loops in the perturbative expansion are cut off below a given momentum scale κ. Normally κ is chosen to be much larger than all relevant physical scale. Because QCD is renormalizable, $\mathcal{L}^{\kappa}_{\rm QCD}$ is form-invariant under changes of κ provided that the coupling constant $\alpha_s(\kappa^2)$ and quark mass parameter $m(\kappa^2)$ are appropriately defined. However, if we insist on choosing the cutoff κ to be as small as hadronic scales then extra (higher twist) contributions will be generated in the effective Lagrangian density:

$$\begin{aligned}\mathcal{L}^{\kappa} = \mathcal{L}^{\kappa}_0 + \frac{em(\kappa)}{\kappa^2}\,\bar\psi_N\,\sigma_{\mu\nu}\partial^\mu\psi_N A^\nu_{\rm em} + e\,\frac{f_\pi^2}{\kappa^2}\,\phi_\pi^\dagger\partial_\mu\phi_\pi A^\mu_{\rm em} \\ + e\,\frac{f_p^2}{\kappa^2}\,\bar\psi_N\,\gamma_\nu\psi_N A^\nu_{\rm em} + \frac{f_p^2 f_\pi}{\kappa^6}\,\partial_\nu\bar\psi_N\,\gamma_5\gamma^\nu\psi_N\phi_\pi + \cdots\end{aligned} \tag{38}$$

where $\mathcal{L}^{\kappa}_0$ is the standard Lagrangian and the "higher twist" terms of order κ^{-2}, κ^{-4}, ... are schematic representations of the quark Pauli form factor, the pion and nucleon Dirac form factors, and the $\pi - N - N$ coupling. The pion and nucleon fields ϕ_π and ψ_N represent composite operators constructed and normalized from the valence Fock amplitudes and the leading interpolating quark operators. One can use eq. (38) to estimate the effective asymptotic power law behaviors of the couplings, e.g., $F^{\rm quark}_{\rm Pauli} \sim 1/Q^2$, $F_\pi \sim f_\pi^2/Q^2$, $G_M \sim f_p^2/Q^4$ and the effective $\pi\bar N\,\gamma_5 N F_{\pi N\bar N}$ coupling: $F_{\pi N\bar N}(Q^2) \sim M_N f_p^2 f_\pi/Q^6$.

The net pion exchange amplitude for $NN-NN$ scatterings thus falls off very rapidly at large momentum transfer $M^{\pi}_{NN\to NN} \sim (Q^2)^{-7}$ much faster than the leading quark interchange amplitude $M^{q\bar{q}}_{NN\to NN} \sim (Q^2)^{-4}$. Similarly, the vector exchange contributions give contributions $M^{\rho}_{NN\to NN} \sim (Q^2)^{-6}$. Thus meson exchange amplitudes and currents, even summed over their excited spectra, do not contribute to the leading asymptotic behavior of the $N-N$ scattering amplitudes or deuteron form factors once proper account is taken of the off-shell form factors which control the meson-nucleon-nucleon vertices.

Aside from such estimates, the effective Lagrangian, eq. (38) only has utility as a rough tree graph approximation; in higher order the hadronic field terms give loop integrals highly sensitive to the ultraviolet cutoff because of their non-renormalizable character. Thus an effective meson-nucleon Lagrangian serves to organize and catalog low energy constraints and effective couplings, but it is not very predictive for obtaining the actual dynamical and off-shell behavior of hadronic amplitudes due to the internal quark and gluon structure.

Local Lagrangians field theories for systems which are intrinsically composite are however misleading in another respect. Consider the low-energy theorem for the forward Compton amplitude on a (spin-average) nucleon target

$$\lim_{\nu \to 0} M_{\gamma p\to\gamma' p}(\nu, t=0) = -2\,\hat{\epsilon}\cdot\hat{\epsilon}'\,\frac{e^2}{M_p}\ . \tag{39}$$

One can directly derive this result from the underlying quark currents as indicated in fig. 15(b). However, if one assumes the nucleon is a local field, then the entire contribution to the Compton amplitude at $\nu = 0$ would arise from the nucleon pair z-graph amplitude, as indicated in fig. 15(a). Since each calculation is Lorentz and gauge invariant, both give the desired result, eq. (39). However, in actuality, the nucleon is composite and the $N\bar{N}$ pair term is strongly suppressed: each $\gamma p\,\bar{p}$ vertex is proportional to

$$\langle 0|J^{\mu}(0)|p\,\bar{p}\rangle \propto F_p(Q^2 = 4M_p^2)\ ; \tag{40}$$

i.e., the timelike form factor as determined from $e^+e^- \to p\bar{p}$ near threshold. Thus, as would be expected physically, the $N\bar{N}$ pair contribution is highly suppressed for a composite system (even for real photons). Clearly a Lagrangian based on local nucleon fields gives an inaccurate

description of the actual dynamics and cannot be trusted away from the forward scattering, low energy limit.

We can see from the above discussion that a necessary condition for utilizing a local Lagrangian field theory as a dynamical approximation to a given composite system H is that its timelike form factor at the Compton scale must be close to 1:

$$F_H(Q^2 \simeq 4M^2) \simeq 1 \,. \tag{41}$$

For example, even if it turns out that the electron is a composite system at very short distances, the QED Lagrangian will still be a highly accurate tool. Equation (41) fails for all hadrons, save the pion, suggesting that effective chiral field theories which couple point-like pions to quarks could be a viable approximation to QCD.

More generally, one should be critical of any use of point-like couplings for nucleon-antinucleon pair production, e.g., in calculations of deuteron form factors, photo- and electro-disintegration since such contributions are always suppressed by the timelike nucleon form factor. Note $\gamma N \bar{N}$ point-like couplings are not needed for gauge invariance, once all quark current contributions including pointlike $q\bar{q}$ pair terms are taken into account.

We also note that a relativistic composite fermionic system, whether it is a nucleon or nucleus, does not obey the usual Dirac equation—with a momentum-independent potential—beyond first Born approximation. Again, the difficulty concerns intermediate states containing $N\bar{N}$ pair terms: the identity of the Dirac equation requires that $\langle p|V_{\rm ext}|p'\rangle$ and $\langle 0|V_{\rm ext}|p'\,\bar{p}\rangle$ be related by simple crossing, as for leptons in QED. For composite systems the pair production terms are suppressed by the timelike form factor (40). It is however possible that one can write an effective, approximate relativistic equation for a nucleon in an external potential of the form

$$(\vec{\alpha}\cdot\vec{p} + \beta m_N + \Lambda_+ V_{\rm eff}\Lambda_+)\Psi_N = E\Psi_N \tag{42}$$

where the projection operator Λ_+ removes the $N-\bar{N}$ pair terms, and $V^{\rm eff}$ includes the local (seagull) contributions from $q\bar{q}$-pair intermediate states, as well as contributions from nucleon excitation.

An essential property of a predictive theory is its renormalizability, the fact that physics at a very high momentum scale $k^2 > \kappa^2$ has no effect on the dynamics other than to define the effective coupling constant $\alpha(\kappa^2)$ and mass terms $m(\kappa^2)$. Renormalizability also implies that fixed angle unitarity is satisfied at the tree-graph (no-loop) level. In addition, it has recently been shown that the tree graph amplitude for photon emission for any renormalizable gauge theory has the same amplitude zero structure as classical electrodynamics. Specifically, the tree graph amplitude for photon emission caused by the
scattering of charged particles *vanishes* (independent of spin) in the kinematic region where the ratios $Q_i/p_i \cdot k$ for all the external charged lines are identical [36], see section 3. This "null zone" of zero radiation is not restricted to soft photon momentum, although it is identical to the kinematic domain for the complete destructive interference of the radiation associated with classical electromagnetic currents of the external charged particles. Thus the tree graph structure of gauge theories, in which each elementary charged field has zero anomalous moment ($g = 2$) is properly consistent with the classical ($\hbar = 0$) limit. On the other hand, local field theories which couple particles with non-zero anomalous moments violate fixed angle unitarity and the above classical correspondence limit at the tree graph level. The anomalous moment of the nucleon is clearly a property of its internal quantum structure;
by itself, this precludes the representation of the nucleon as a local field.

The essential conflict between quark and meson-nucleon field theory is thus at a very basic level: because of Lorentz invariance a conserved charge must be carried by a local (point-like) current; there is no consistent relativistic theory where fundamental constituent nucleon fields have an extended charge structure.

4.6 NCD conclusions

The synthesis of nuclear dynamics with the quark and gluon processes of quantum chromodynamics is clearly a basic fundamental problem in hadron physics. The short distance behavior of the nucleon-nucleon interaction as determined by QCD must join smoothly and analytically with the large distance constraints of nuclear physics. As we have emphasized, the fundamental mass scale of QCD is comparable with the inverse nuclear radius; it is thus

difficult to argue that nuclear physics at distances below ~ 1 *fm* can be studied in isolation from QCD: meson and nucleon degrees of freedom of traditional nuclear physics models must become inadequate at momentum transfer scales $\gtrsim 200$ MeV where nucleon substructure becomes evident.

Thus the essential question for nuclear as well as particle physics is to understand the transition between the meson-nucleon and quark-gluon degrees of freedom. There should be no illusion that this is a simple task; one is dealing with all the complexities and fascinations of QCD such as the effects of confinement and non-perturbative effects intrinsic to the non-Abelian theory. Such considerations also enter the physics associated with the propagation of quarks and gluons in nuclear matter and the phenomenology of hadron and nuclear wavefunctions [70].

Despite the difficulty of the non-perturbative domain, there is reason for optimism that "nuclear chromodynamics" is a viable endeavor. For example, we can use QCD to make predictions for the short distance behavior of the deuteron wavefunction and the deuteron form factor at large momentum transfer. The predictions give a remarkably accurate description of the scaling behavior of the available deuteron form factor data for Q^2 as low as 1 GeV^2. The QCD approach also allows the definition of "reduced" nuclear amplitudes which can be used to consistently and covariantly remove the effect of nucleon compositeness from nuclear amplitudes. An important feature of such predictions is that they provide rigorous constraints on exclusive nuclear amplitudes which have the correct analytic, gauge-invariant, and scaling properties predicted by QCD at short distances. This suggests the construction of boundary condition model amplitudes which simultaneously satisfy low energy and chiral theorems at low momentum transfer as well as the rigorous QCD constraints at high momentum transfers [71]. In addition, by using the light cone formalism, one can obtain a consistent relativistic Fock state wave function description of hadrons and nuclei which ties on to the Schroedinger theory in the non-relativistic regime. One can also be encouraged by progress in non-perturbative methods in QCD such as lattice gauge theories or chromostatics [72]; eventually these approaches should be able to deal with multiquark
source problems.

It is essential to have direct experiment guidance in how to proceed as one develops nuclear chromodynamics. A high duty factor electron accelerator [73] with laboratory energy beyond 4 GeV is an important tool because of the simplicity of the probe and the fact that we understand the coupling of the electron and quark current in QCD. It is also clear that

1. One must have sufficient energy to extend electron scattering measurements from low momentum transfer to the high momentum transfer region with sufficient production energy such that Bjorken scaling can be observed. One certainly does not want to stop at an intermediate momentum transfer domain—a regime of maximal complexity from the standpoint of both QCD and nuclear physics. The recent EMC and SLAC data showing breakdown of simple nucleon additivity in the nuclear structure functions also demonstrates that there is non-trivial nuclear physics even in the high momentum transfer domain.

2. One must have sufficient electron energy to separate the longitudinal and transverse currents. The σ_L/σ_T separation is essential for resolving individual dynamical mechanisms; e.g., single quark and multiple quark (meson current) contributions.

3. One wishes to study each exclusive channel in detail in order to verify and understand the emergence of QCD scaling laws and to understand how the various channels combine together to yield effective Bjorken scaling. Helicity information is also very valuable. For example QCD predicts that at large momentum transfer, the helicity-0 to helicity-0 deuteron form factor is dominant and that for any large momentum transfer reaction, total hadronic helicity is conserved [57].

4. One wishes to make a viable search for dibaryon states which are dominantly of hidden color. The argument that such resonances exist in QCD is compelling just from counting of degrees of freedom. The calculation of the mass and width of such resonances is clearly very difficult, since the detailed dynamics is dependent on the degree of mixing with ordinary states, the availability of decay channels, et cetera. Since hidden color states have suppressed overlap with the usual hadronic amplitudes it may be quite difficult to find such states in ordinary hadronic collisions. On the other hand, the virtual photon probe gives a hard momentum transfer to a single struck quark, and

it is thus more likely to be sensitive to the short-distance hidden color components in the target wave function. Adequate electron energy is essential not only to produce dibaryon resonances but also to allow sufficient momentum transfer Q^2 to decrease backgrounds and to provide σ_L/σ_T separation.

5. One wishes to probe and parametrize the high momentum transfer dependence of the deuteron $n-p$ and $\Delta-\Delta$ components, as a clue toward a complete description of the nuclear wavefunction.

6. One wishes to measure the neutron, pion, and kaon form factors.

7. The region well beyond $x = 1$ for deep inelastic electron-nucleus scattering is important QCD physics since the virtual quark and gluon configurations in the nuclear wave function are required to be far off shell. Understanding the detailed mechanisms which underlie this dynamics will require coincident measurements and the broadest kinematic region available for σ_L/σ_T separation. The y-variable approach which attributes the electron scattering to nucleon currents is likely to break down even at moderate Q^2. Coincidence measurements which can examine the importance of the nucleon component are well worth study.

8. One wishes to study the emergence of strangeness in the nuclear state.

The fact that QCD is a viable theory for hadronic interactions implies that a fundamental description of the nuclear force is now possible. Although detailed work on the synthesis of QCD and nuclear physics is just beginning, it is clear from the structure of QCD that several traditional concepts of nuclear physics will have to be modified. These include conventional treatments of meson and baryon-pair contributions to the electromagnetic current and analyses of the nuclear form factor in terms of factorized on-shell nucleon form factors. On the other hand, the reduced nuclear form factor and scattering matrix elements give a viable prescription for the extrapolation of nuclear amplitudes to zero nucleon radius. There is thus the possibility that even the low momentum transfer phenomenology of nuclear parameters will be significantly modified.

Acknowledgments

Many of the results presented here are based on collaborations with E. L. Berger, G. Bodwin, R. Brown, J. R. Hiller, T. Huang, C-R. Ji, K. L. Kowalski, G. P. Lepage, and P. B. Mackenzie. Part of this talk was also presented at the 3rd International Conference on Physics in Collisoiins, Como, Italy (1983) and the Tenth International Conference on Few Body Problems in Physics, Karlsruhe, Germany (1983).

Appendix: Automatic scale setting [12]

One of the most serious problems confronting the quantitative interpretation of QCD is the ambiguity concerning the setting of the scale in perturbative expansions. As an example, consider the standard perturbative expansion for the e^+e^- annihilation cross section in ($\overline{MS}$ scheme)

$$\left[\frac{R_{e^+e^-}(Q^2)}{3\sum e_q^2}-1\right]=\frac{\alpha_s^{\overline{MS}}(Q^2)}{\pi}\left[1+(1.98-0.115\,n_f)\frac{\alpha_s}{\pi}+O\left(\frac{\alpha_s^2}{\pi^2}\right)+\cdots\right]. \tag{43}$$

were n_f is the number of light fermion flavors with $m_f^2 \ll Q^2$. Note that if one chooses a different scale $Q \to \kappa Q$ in the argument $\alpha_s^{\overline{MS}}$ then the coefficient of all subsequent terms are changed. If this were a true ambiguity of QCD then higher order perturbative coefficients are not well-defined; furthermore, there is no clue toward the convergence rate of the expansion.

Is the scale choice really arbitrary? Certainty it is not arbitrary in QED. The running coupling constant is defined as

$$\alpha(Q^2)=\frac{\alpha(Q_0^2)}{1-\alpha(Q_0^2)[\pi(Q^2)-\pi(Q_0^2]} \tag{44}$$

where $\pi(Q^2)$ sums the proper contributions to the vacuum polarization. In lowest order QED

$$\pi(Q^2)-\pi(Q_0^2)\simeq n_f\frac{\alpha}{3\pi}\log\frac{Q^2}{Q_0^2}\,. \tag{45}$$

The use of the running coupling constant simplifies the form of QED perturbative expansions. For example, the light flavor contributions to the muon anomalous moment is automatically summed when we use the form

$$a_\mu=\frac{\alpha(Q^*)}{2\pi}+0.327\ldots\frac{\alpha^2(Q^*)}{\pi^2}+\cdots \tag{46}$$

where the scale Q^* is chosen such that [74]

$$\alpha(Q^*)=\frac{\alpha}{1-\frac{\alpha}{\pi}\left(\frac{2}{3}\log\frac{m_\mu}{m_e}-\frac{25}{18}\right)+\cdots}\,. \tag{47}$$

The scale Q^* in eq. (46) is in fact unique; it is defined via eq. (47) in such a way as to automatically sum all vacuum polarization contributions. The form of eq. (46) is invariant

as one changes the overall scale (e.g., $m_\mu \to m_\tau$) as we pass each new flavor threshold, if the vacuum polarization contribution of each new flavor is included in (47). Note, however, that the light-by-light contribution to a_μ, which appears in order α^3/π^3 from light-flavor box graphs, is not included in $a_\mu(Q^*)$ since this contribution is not part of the photon propagator renormalization and it does not contribute as a geometric series in higher order. Furthermore, for some QED processes, e.g., orthopositronium decay

$$\Gamma_{\text{orthopositronium}\to 3\gamma} \propto \alpha^3 m_e\left[1 - 10.3\,\frac{\alpha}{\pi} + \cdots\right] \tag{48}$$

there are no vacuum polarization corrections to this order, so the large coefficient cannot be avoided by resetting the scale in α. In QED, the running coupling constant simply sums $\alpha(Q)$ vacuum polarization contributions; in effect there are no scale-ambiguities for setting the scale. Similarly in QCD, it must be true that the vacuum polarization due to light fermions should be summed in $\alpha_s(Q)$. In fact, as we show below, this natural requirement automatically and consistently fixes the QCD scale for the leading non-trivial order in α_s for most QCD processes of interest.

In QCD the running coupling constant satisfies

$$\alpha_s(Q^*) = \frac{\alpha_s(Q)}{\left[1 + \frac{\beta_0}{2\pi}\alpha_s(Q)\ell n\left(\frac{Q^*}{Q}\right) + \cdots\right]} \tag{49}$$

where $\beta_0 = 11 - 2/3\,n_f$. Consider any observable $\rho(Q)$ which has a perturbative expansion at large momentum transfer Q. For definiteness we choose the $\overline{MS}$ renormalization scheme to define the renormalization procedure, and adopt the canonical form,

$$\rho(Q) = \frac{\alpha_{\overline{MS}}(Q)}{\pi}\left[1 + \frac{\alpha_{\overline{MS}}}{\pi}(A_{vp}n_f + B) + \cdots\right].$$

The second order coefficient can also be written as $-\frac{3}{2}\beta_0 A_{vp} + \left(\frac{33}{2}A_{vp} + B\right)$. The requirement that the fermion vacuum polarization contribution is absorbed into the running coupling constant plus the fact that $\alpha(Q)$ is a function of n_f through β_0 then uniquely sets the scale of the leading order coefficient:

$$\rho(Q) = \frac{\alpha_{\overline{MS}}(Q^*)}{\pi}\left[1 + \frac{\alpha_{\overline{MS}}}{\pi}C_1 + \cdots\right] \tag{50}$$

where $Q^* \equiv Q\, e^{3A_{vp}}$ and $C_1 = B + \frac{33}{2} A_{vp}$. For example, from eq. (2.1) we have

$$\rho_R(Q) \equiv \left(\frac{R_{e^+e^-}(Q^2)}{3\Sigma e_q^2} - 1\right) = \frac{\alpha_{\overline{MS}}(0.71\,Q)}{\pi}\left[1 + 0.08\,\frac{\alpha_{\overline{MS}}}{\pi} + \cdots\right]. \tag{51}$$

Thus Q^* and C_1 are determined unambiguously within this renormalization scheme and are each n_f-independent. Note that the expansion is unchanged in form as one passes through a new quark threshold. Given any renormalization scheme, the above procedure automatically fixes the scale of the leading order coefficient for the non-Abelian theory. In higher orders one must carefully identify the correct $n_f\, A_{vp}$ terms; e.g., distinguish light-by-light or trigluon fermion loop contributions not associated with the definition of $\alpha_s(Q)$.

If we apply the procedure (50) to the QCD interaction potential between heavy quarks, then one obtains

$$V(Q) = -C_F \frac{4\pi\, \alpha_{\overline{MS}}(Q^*)}{Q^2}\left[1 - 2\frac{\alpha_{\overline{MS}}}{\pi} + \cdots\right] \tag{52}$$

where $Q^* = e^{-5/6}\, Q \cong 0.43Q$. Thus the effective scale Q^* in $\overline{MS}$ is $\sim 1/2$ of the "true" momentum transferred by $V(Q)$.

The results (51), (52) suggest that $R_{e^+e^-}$ or $V(Q)$ can be used to define and normalize $\alpha_s(Q)$. Such empirical definitions serve as a renormalization scheme alternative to $\overline{MS}$. For example, in principle we can define

$$\frac{\alpha_R(Q)}{\pi} \equiv \left[\frac{R_{e^+e^-}(Q)}{3\Sigma e_q^2} - 1\right] \tag{53}$$

as a physical definition of $\alpha_s(Q)$ analogous to the Coulomb scattering definition of α in QED. Note then that $\alpha_R(Q)$ and $\alpha_{\overline{MS}}(0.71\,Q)$ are effectively interchangeable.

A further benefit of the "automatic scale fixing procedure" is that the physical characteristics of the effective scale can be understood. For example, the evolution of the non-singlet moments is uniquely written in the form

$$\frac{\partial}{\partial \ell n\, Q^2} \ell n\, M_n(Q^2) = -\frac{\gamma_n^0}{8\pi}\alpha_{\overline{MS}}(Q^*)\left[1 - \frac{\alpha_{\overline{MS}}(Q_n^*)}{\pi} C_n + \cdots\right] \tag{54}$$

with

$$\begin{aligned} Q_2^* &= 0.48\,Q\,, \quad C_2 = 0.27 \\ Q_{10}^* &= 0.21\,Q\,, \quad C_{10} = 1.1 \end{aligned} \tag{55}$$

and $Q_n^* \sim Q/\sqrt{n}$ for large n. This dependence on $\sqrt{n}$ reflects the physical fact that the phase space limit on the gluon radiation causing the Q^2-evolution decreases in the large n, $x \to 1$ regime.

In the case of Υ decay, the scale-fixed form of the Lepage-Mackenzie [12] calculation is

$$\frac{\Gamma(\Upsilon \to hadrons)}{\Gamma(\Upsilon \to \mu^+\mu^-)} = \frac{10(\pi^2-9)}{81\pi e_b^2} \frac{\alpha_{\overline{MS}}(Q^*)}{\alpha_{QED}^2}\left(1 - \frac{\alpha_{\overline{MS}}}{\pi}(14.0 \pm 0.5) + \cdots\right) \tag{56}$$

where $Q^* = 0.157 M_\Upsilon$. Thus, just as in the case for orthopositronium, a large second order coefficient is unavoidable. Other procedures which reduce or eliminate this coefficient by an ad hoc procedure are clearly incorrect if they are invalid in QED.

A very useful process for automatic scale setting is the photon branching ratio.

$$\frac{\Gamma(\Upsilon \to \gamma_D + hadrons)}{\Gamma(\Upsilon \to hadrons)} = \frac{36\, e_b^2}{5} \frac{\alpha_{QED}}{\alpha_{\overline{MS}}(Q^*)}\left[1 + \frac{\alpha_{\overline{MS}}(Q^*)}{\pi}(2.2 \pm 0.6) + \cdots\right] \tag{57}$$

where again $Q^* = 0.157\ M_\Upsilon$.

The automatic scale setting procedure should have general utility for evaluating the natural scale in a whole range of physical processes. In the case of some reactions such as hadron production $H_A H_B \to H_C X$ at large p_T each parton structure function has its own scale $\sim Q^2(1-x_i)$. In addition each hard scattering amplitude has a scale determined by corresponding fermion loop vacuum polarization contributions.

References

1. Reviews of QCD are given in A. J. Buras, Rev. Mod. Phys. 53, 199 (1980); A. H. Mueller, Phys. Rep. 73C, 237 (1981); and E. Reya, Phys. Rept. 69, 195 (1981).

2. G. P. Lepage, S. J. Brodsky, T. Huang and P. B. Mackenzie, in the Proc. of the Banff Summer Institute on Particle Physics, Alberta, Canada; S. J. Brodsky, in Quarks and Nuclear Forces, Springer 100 (1981).

3. A review of higher twist contributions is given by S. J. Brodsky, E. L. Berger, and G. P. Lepage, Proceedings of the Drell-Yan Workshop, FNAL (1982). See also R. K. Ellis, W. Furmanski, and R. Petronzio, CERN-TH-3301 (1982) and R. Blankenbecler, S. J. Brodsky, and J. F. Gunion, Phys. Rev. D18, 900 (1978).

4. G. T. Bodwin, S. J. Brodsky, and G. P. Lepage, Phys. Rev. Lett. 47, 1799 (1983) and SLAC-PUB-2966, published in the proceedings of the XIII International Symposium on Multiparticle Dynamics, Volendam, The Netherlands (1982), SLAC-PUB-2860, to be published in the Proceedings of the Banff Summer School on Particles and Fields, 1981.

5. W. W. Lindsay, D. A. Ross, and C. T. Sachrajda, Phys. Lett. 117B, 105 (1982), Nucl. Phys. B, 214 (1983), and Southampton preprint 82/83-4 (1983).

6. Outlines of general all–orders proofs are given in J. C. Collins, D. Soper, and G. Stevinson, Ill. Tech. preprint (1983), and G. Bodwin, S. J. Brodsky and G. P. Lepage (in preparation).

7. G. P. Lepage and S. J. Brodsky, Phys. Rev. D22, 2157 (1980); S. J. Brodsky and G. P. Lepage, SLAC-PUB-2294, published in "Quantum Chromodynamics," edited by Wm. Frazer and F. Henyey (AIP, 1979), Phys. Lett. 87B, 359 (1979); S. J. Brodsky, Y. Frishman, G. P. Lepage and C. Sachrajda, Phys. Lett. 91B, 239 (1980). See also A. V. Efremov and A. V. Radyushkin, Rev. Nuovo Cimento 3, 1 (1980), Phys. Lett. 94B, 245 (1980); A. Duncan and A. Mueller, Phys. Rev. D21, 1636 (1980), Phys. Lett. 90B, 159 (1980); G. R. Farrar and D. R. Jackson, Phys. Rev. Lett. 43, 246 (1979); V. L. Chernyak and A. R. Vhitnishii, JETP Lett. 25, 11 (1977); G. Parisi, Phys. Lett.

43, 246 (1979); M. K. Chase, Nucl. Phys. B167, 125 (1980). V. N. Baier and A. G. Grozin, Nucl. Phys. B192, 476 (1981).

8. For additional discussion of applications of QCD to nuclear physics and references, see S. J. Brodsky, published in the proceedings of the conference "New Horizons in Electromagnetic Physics", University of Virginia, April 1982; S. J. Brodsky, T. Huang and G. P. Lepage, SLAC-PUB-2868 (1982) published in Springer Tracts in Modern Physics, Vol. 100, "Quarks and Nuclear Forces", ed. D. Fries and B. Zeitnitz (1982); S. J. Brodsky and G. P. Lepage, in the proceedings of the Eugene Few Body Conference 1980: 247C (Nucl. Phys. A363, 1981) and S. J. Brodsky, to be published in the proceedings of the NATO Pacific Summer Institute Progress in Nuclear Dynamics, Vancouver Island (1982).

9. For a recent discussion of progress in the derivation of nuclear forces from QCD-based models, see K. Maltman and N. Isgur, Phys. Rev. Letters 50, 1827 (1983), E. L. Lomon, MIT preprint CTP No. 1116 (1983); and references therein. The quark interchange mechanism for $N-N$ scattering is discussed in J. F. Gunion, S. J. Brodsky, and R. Blankenbecler, Phys. Rev. D8, 287 (1983). Qualitative QCD-based arguments for the repulsive $N-N$ potential at short distances are given in C. Detar, HU-TFT-82-6 (1982); M. Harvey (Ref. 7); R. L. Jaffe, Phys. Rev. Lett. 24, 228 (1983); and G. E. Brown, in Erice 1981, Proceedings, Quarks and the Nucleus. The possibility that the dueteron form factor is dominated at large momentum transfer by hidden color components is discussed in V. A. Matveev and P. Sorba, Nuovo Cimento 45A, 257 (1978); Nuovo Cimento 20, 435 (1977).

10. R. T. Aubert, et al., Phys. Lett. 105B, 315, 322 (1981); Phys. Lett. 123B, 123, 275 (1983). A. Bodek, et al., Phys. Rev. Lett. 50, 1431; 51, 524 (1983). For recent theoretical discussions and references to the EMC effect see e.g., M. Chemtob and R. Peschanski, Saclay preprint SPh.T/83/116 (1983), and E. Lomon (this proceedings). Various models are discussed in H. J. Pirner and J. P. Vary, Phys. Rev. Lett. 46, 1376 (1981); R. Jaffe, Phys. Rev. Lett. 50, 228 (1983). L. S. Celenza and C. Shakin, Brooklyn College preprint BCINT-82/111/117 (1982). M. Staszel, J. Roznek, G. Wilk,

Warsaw preprint IFT19/83 (1983). F. E. Close, R. B. Robert, G. G. Ross, Rutherford preprint RL-83-051 (1983). O. Nachtmann and J. H. Pirner, Heidelberg preprint HD-THE-8-83-8 (fi983).

11. For a review, see Y. Karant, LBL preprint (1983).

12. S. J. Brodsky, G. P. Lepage and P. Mackenzie, Phys. Rev. D28, 228 (1983).

13. This section is based on collaborations with G. T. Bodwin and G. P. Lepage and was also presented at the Workshop on Nonperturbative QCD, Oklahoma State University, March (1983). See also G. T. Bodwin, S. J. Brodsky and G. P. Lepage, Ref. 14. The first calculations of color correlations in two-loop order were incomplete because of contributions outside the Glauber region.

14. S. D. Drell and T. M. Yan, Phys. Rev. Lett. 25, 316 (1970).

15. J. C. Collins and D. E. Soper, Proceedings of the Moriond Workshops, Les Arce, France (1981).

16. J. E. Ellis, M. K. Gaillard and W. J. Zakrzewski, Phys. Lett. 81B, 224 (1979).

17. J. Frenkel *et al.*, preprint IFUSP/P-405 (1983), and references therein.

18. See e.g., F. Khalafi and J. Stirling, Cambridge preprint DAMTP 83/2 (1983). For reviews, see J. Stirling in Proceedings of the XIIIth International Symposium on Multiparticle Dynamics, Volendam (1982).

19. L. Landau and I. Pomeranchuk, Dok. Akademii Nauk SSSR 92, 535 (1953), and 92, 735 (1953); L. Stodolsky, MPI-PAE/pTH 23/75 (1981); I. M. Dremin, Lebedev preprint 250 (1981).

20. A. Mueller, Phys. Lett. 108B, 355 (1982); A. Sen and G. Sterman, FermilabPUB-83/42 ThY (1983).

21. J. C. Collins, D. E. Soper and G. Sterman, Phys. Lett. 109B, 288 (1983), SUNY preprint ITP-SB-82-46 (1982); A. V. Efremov and A. V. Radyushkin, Theor. Math. Phys. 44, 664 (1981).

22. For related work, see also J. C. Collins, D. E. Soper and G. Sterman, Phys. Lett. 126B, 275 (1983).

23. A. Mueller, Proceedings of the Drell-Yan Workshop, FNAL (1982).

24. G. P. Lepage and S. J. Brodsky, Phys. Rev. D22, 2157 (1980).

25. E. L. Berger and S. J. Brodsky, Phys. Rev. D 24, 2428 (1981); J. A. Bagger and J. F. Gunion, Phys. Rev. D 25, 2287 (1982), and UCD-82/1 (1983); S. J. Brodsky and J. Hiller, Phys. Rev. C 28, 475 (1983).

26. This has been discussed by A. H. Mueller, to be published in Proceedings of the Moriond Conference (1982). Applications to elastic hadron-nucleus amplitudes are given in S. J. Brodsky and B. T. Chertok, Phys. Rev. Lett. 37, 269 (1976). Color singlet cancellations for valence states interacting inclusively in nuclei are discussed in G. Bertsch, S. J. Brodsky, A. S. Goldhaber and J. F. Gunion, Phys. Rev. Lett. 47, 297 (1981). Further discussion may be found in S. J. Brodsky, SLAC-PUB-2970 (1982), published in the Proceedings of the XIIIth International Symposium on Multiparticle Dynamics, Volendam, The Netherlands (1982), and Ref. 19.

27. G. R. Farrar and D. R. Jackson, Phys. Rev. Lett. 35, 1460 (1975); E. L. Berger and S. J. Brodsky, Phys. Rev. Lett. 42, 940 (1979).

28. B. Pire and J. Ralston, in Proceedings of the Drell-Yan Workshop, FNAL, 1983.

29. J. D. Bjorken, lecture notes in *Current-Induced Reactions*, edited by J. Komer *et al.*, Springer-Verlag (New York) 1975; J. Kogut and L. Susskind, Phys. Rev. D 10, 732 (1974).

30. S. J. Brodsky, SLAC-PUB-2395, also in Proceedings of the First Workshop on Nuclear Collisions, Berkeley (1979). and references therein.

31. See J. Kühn, Phys. Rev. D 13, 2948 (1976); and A. Krzywicki, J. Engels, B. Petersson and V. Sukhatme, Phys. Lett. 85B, 407 (1979),

32. N. Paver and D. Treleani, Nuovo Cimento A70, 215 (1982); S. J. Brodsky and J. F. Gunion (unpublished); B. Humbert, CERN-TH-3620

33. G. Bertsch, S. J. Brodsky, A. S. Goldhaber and J. F. Gunion, Ref. 21.

34. F. Vanucci, Contribution to the Karlsruhe Summer Institute, Karlsruhe (1978).

35. R. W. Brown, D. Sahdev and K. O. Mikaelian, Phys. Rev. D 20, 1164 (1979); K. O. Mikaelian, M. A. Samuel and D. Sahdev, Phys. Rev. Lett. 43, 746 (1979); K. O. Mikaelian, Phys. Rev. D 17, 750 (1978).

36. S. J. Brodsky and R. W. Brown, Phys. Rev. Lett. 49, 966 (1982); R. W. Brown, K. L. Kowalski and S. J. Brodsky, Phys. Rev. D 28, 624 (1983).

37. See also M. A. Samuel, Phys. Rev. D 27, 2724 (1983).

38. V. Bargmann, L. Michel and V. L. Telegdi, Phys. Rev. Lett. 2, 435 (1959); S. J. Brodsky and J. R. Primack, Ann. Phys. (N.Y.) 52, 315 (1969).

39. See, e.g. M. L. Laursen, M. A. Samuel and A. Sen, Phys. Rev. D 28, 650 (1983); N. M. Royomleo and J. H. Reed, preprint TRI-PP-83-33 (1983).

40. G. Passarino, SLAC-PUB-3024 (1982), to appear in Nucl. Phys. B224.

41. G. P. Lepage and S. J. Brodsky, Phys. Rev. D22, 2157 (1980).

42. E. L. Berger, S. J. Brodsky, and G. P. Lepage, SLAC–PUB–3027 published in the Proc. of the Workshop on Drell–Yan Processes, FNAL (1982).

43. J. P. Ralston and B. Pine, ANL–NEP–C8–82–67 (1982), published in the Proc. of the Workshop on Drell-Yan Processes, FNAL (1982).

44. J. F.Gunion, P. Nason and R. Blankenbecler, Phys. Lett. 117B, 353 (1982), and SLAC–PUB–3142 (1983).

45. L. F. Abbott, W. B. Attwood, R. M. Barnett, Phys. Rev. D22, 582 (1982). I. A. Schmidt and R. Blankenbecler, Phys. Rev. D16, 1318 (1977).

46. For a review, see F. Halzen, Journal de Physique, Colloque C3, supp #12, Tome 43, Dec 1982.

47. S. J. Brodsky, C. Peterson, N. Sakai, Phys. Rev. D23, 2745 (1981); S. J. Brodsky, P. Hoyer, C. Peterson, N. Sakai, Phys. Lett. 93B, 451 (1980).

48. See, e.g. G. Adkins, C. R. Nappi, and E. Witten, Princeton preprint (1983); G. E. Brown, Nucl. Phys. A374, 63C (1982); C. Shakin, Brooklyn College preprint 82/081/115; M. C. Birse and M. K. Banerjee, University of Maryland preprint 83-201.

49. S. J. Brodsky, C.-R. Ji, G. P. Lepage, Phys. Rev. Lett. 51, 83 (1983).

50. C. Klopfenstein, et al., CUSB 83-07 (1983).

51. S. J. Brodsky, G. P. Lepage, P. B. Mackenzie, Phys. Rev. D28, 228 (1983).

52. Details of light-cone Fock methods are given in G. P Lepage, S. J. Brodsky, T. Huang, and P. B. Mackenzie CLNS-82/522, published in proceedings of the Banff Summer Institute on Particle Physics, Alberta, Canada, S. J. Brodsky and G. P. Lepage, Phys. Rev. D24, 1808 (1981) and S. J. Brodsky, in proceeding of Quarks and Nuclear Forces, Springer 100, Bad Liebenzell (1981).

53. S. J. Brodsky and G. P. Lepage, Phys. Rev. Lett. 43, 545, 1625(E) (1979). S. J. Brodsky, G. P. Lepage, S.A.A. Zaidi, Phys. Rev. D23, 1152 (1981).

54. S. J. Brodsky and B. T. Chertok, Phys. Rev. Lett. 37, 269 (1976); Phys. Rev. D14, 3003 (1976). S. J. Brodsky, in Proceedings of the International Conference on Few Body Problems in Nuclear and Particle Physics, Laval University, Quebec (1974).

55. S. J. Brodsky and J. R. Hiller, Phys. Rev. C28, 475 (1983). Figure 6 is corrected for a phase-space factor $\sqrt{s/(s-m_d^2)}$.

56. S. J. Brodsky and G. R. Farrar, Phys. Rev. Lett. 31, 1153 (1973), and Phys. Rev. D11, 1309 (1975); V. A. Matveev, R. M. Muradyan and A. V. Tavkheldize, Lett. Nuovo Cimento 7, 719 (1973).

57. S. J. Brodsky and G. P. Lepage, Phys. Rev. D24, 2848 (1981).

58. M. D. Mestayer, SLAC-Report 214 (1978) F. Martin, et al., Phys. Rev. Lett. 38, 1320 (1977); W. P. Schultz, et al., Phys. Rev. Lett. 38, 259 (1977); R. G. Arnold, et al., Phys. Rev. Lett. 40, 1429 (1978); B. T. Chertok, Phys. Lett. 41, 1155 (1978); D. Daty, et al., Phys. Rev. Lett. 43, 1143 (1979). Summaries of the data for nucleon and nuclear form factors at large Q^2 are given in B. T. Chertok, in Progress in Particle and Nuclear Physics, Proceeding of the International School of Nuclear Physics,

5th Course, Erice (1978), and Proceedings of the XVI Rencontre de Moriond, Les Arcs, Savoie, France, 1981.

59. H. J. Behrend, et al., CELLO collaboration preprint (1983). W. J. Stirling, DAMTP 83/17 to be published in the proceedings of the 5th International Workshop on Photon-Photon Collisions (1983).

60. S. J. Brodsky and G. P. Lepage, Phys. Rev. D24, 1808 (1981).

61. S. J. Brodsky, T. Huang, G. P. Lepage, SLAC-PUB-2540 (1980), and T. Huang, SLAC-PUB-2580 (1980), published in the Proceedings of the XXth International Conference on High Energy Physics, Madison, Wisconsin (1980).

62. S. J. Brodsky, C.-R. Ji, and G. P. Lepage (to be published).

63. See also A. Matveev and P. Sorba, reference 3.

64. G. R. Farrar and F. Neri, Rutgers preprint RU-83-20 (1983).

65. M. Harvey, Nucl. Phys. A352, 301, 326 (1981).

66. S. J. Brodsky, C.-R. Ji and G. P. Lepage (to be published).

67. A more detailed discussion of the material of this section is given in S. J. Brodsky, to be published in the proceedings of the NATO Pacific Summer Institute "Progress in Nuclear Dynamics", Vancouver Island (1982).

68. M. Harvey, Nucl. Phys. A352, 301, 326 (1981).

69. See the proceedings of the meeting "New Horizons in Electromagnetic Physics", Virginia (1983).

70. For a discussion and references to QCD effects of quarks and hadrons in nuclear matter, see reference 29 and S. J. Brodsky, SLAC-PUB-3219 (to be published in the proceedings of the Third International Conference on "Physics in Collisions", Como, Italy (1983).

71. For related methods see, e.g. P. Hoodbhoy and L. S. Kisslinger, Carnegie-Mellon preprint (1983). V. G. Ableev, et al., JINR preprint E1-83-487 (1983).

72. S. Adler, IAS preprint (1983), to be published in the proceedings of the Workshop on Non-perturbative QCD. J. Hiller, Ann. Phys. 144, 58 (1982).

73. P. Barnes, et al., NSAC Subcommittee report (1983).

74. This procedure for QED is equivalent to mass-singularity analyses and renormalization group methods discussed by T. Kinoshita, Nuovo Cimento 51B, 140 (1967); B. E. Lautrup and E. deRafael, Nucl. Phys. B70, 317 (1974); and M. A. Samuel, Phys. Rev. D9, 2913 (1978). A related method for summing higher-loop QCD contributions to structure function moments in deep inelastic scattering is given in M. Moshe, Phys. Rev. Lett. 43, 1851 (1979).

Figure Captions

Figure 1 (a) Gluon emission associated with QCD evolution of structure functions for in the Drell-Yan process, $p\bar{p} \to \mu^+\mu^- X$. (b) Gluon emission associated with initial state interactions for the Drell-Yan process. The shaded area represents elastic and inelastic scattering of the incident quarks.

Figure 2 (a) Representation of initial state interactions in perturbative QCD. (b) Simplest example of induced radiation by initial state interactions in $q\pi \to \ell\bar{\ell}X$. Two different physical radiation process are included in this Feynman amplitude depending on whether the intermediate state before or after the gluon emission is on-shell. The two bremsstrahlung processes destructively interfere at energies large compared to a scale in proportional to the target length L.

Figure 3 (a) Representation of initial state interactions in the Drell-Yan cross section $d\sigma/dQ^2dx$. (b) Example of two-loop initial state interactions which cancel by unitarity in an Abelian gauge theory. In QCD these two contributions have different color factors.

Figure 4 Representative active spectator initial state interactions for $\pi\pi \to \ell\bar{\ell}X$ in QCD involving $C_F C_A$ evaluated in Feynman gauge. The real part of the two loop contributions represented by (a),(b), (c) (including mirror diagrams) vanishes at high energies. The imaginary parts cancel against the gluon emission contribution represented in (d) and (e).

Figure 5 (a) Schematic representation of the general decomposition required to prove weak factorization to general orders in QCD. The dotted line corresponds to the eikonal line integral of eq. (10). Vertex corrections which modify the hard scattering amplitude are not shown. These provide a separate factor on the right hand side of 7(a). (b) The relationship between Drell- Yan and deep inelastic lepton scattering eikonal-extended structure functions required to prove factorization.

Figure 6 The differential cross-section for $u\bar{d} \to W^+\gamma$ for $SU(2) \times U(1)$ gauge theory in Born approximation. The subprocess cross section vanishes identically near $\cos\theta^{\gamma d} = 1/3$.

Figure 7 Kinematics for the null zone for $e^-e^- \to e^-e^-\gamma$.

Figure 8 (a) Factorization of the nucleon form factor at large Q^2 in QCD. The optimal scale $\tilde{Q}$ for the distribution amplitude $\phi(x, \tilde{Q})$ is discussed in reference 50. (b) The leading order diagrams for the hard scattering amplitude T_H. The dots indicate insertions which enter the renormalization of the coupling constant. (c) The leading order diagrams which determine the Q^2 dependence of $\phi_B(x, Q)$.

Figure 9 Comparison of experiment with the QCD dimensional counting rule $(Q^2)^{n-1}F(Q^2) \sim const$ for form factors. The proton data extends beyond 30 GeV^2 (see reference 58).

Figure 10 Factorization of the deuteron form factor at large Q^2.

Figure 11 (a) Comparison of the asymptotic QCD prediction (31) with experiment (16) using $F_N(Q^2) = (1 + Q^2/0.71\,GeV^2)^{-2}$. The normalization is fit at $Q^2 = 4\ GeV^2$.

(b) Comparison of the prediction $[1 + (Q^2/m_0^2)]\, f_d(Q^2) \propto (\ell n Q^2)^{-1-2/5\ C_F/\beta}$ with data. The value $m_0^2 = 0.28\ GeV^2$ is used.

Figure 12 Schematic representation of the deuteron wavefunction in QCD indicating the presence of hidden color six-quark components at short distances.

Figure 13 Comparison of deuteron photodisintegration data [76] with the scaling prediction (35) which requires $f^2(\theta_{cm})$ to be independent of energy at large momentum transfer.

Figure 14 Critique of the standard nuclear physics approach to the deuteron form factor at large Q^2. (a) The effective nucleon form factor has one or both legs off shell: $|p_1^2 - p_2^2| \sim q^2/2$. (b) Meson exchange currents are suppressed in QCD because of off shell form factors. (c) The nucleon pair contribution is suppressed because of nucleon compositeness. Contact terms appear only at the quark level.

Figure 15 Time-ordered contributions to (a) The Compton amplitudes in a local Lagrangian theory such as QED. Only the Z-graphs contribute in the forward low energy limit. (b) Calculation of the Compton amplitude for composite systems.

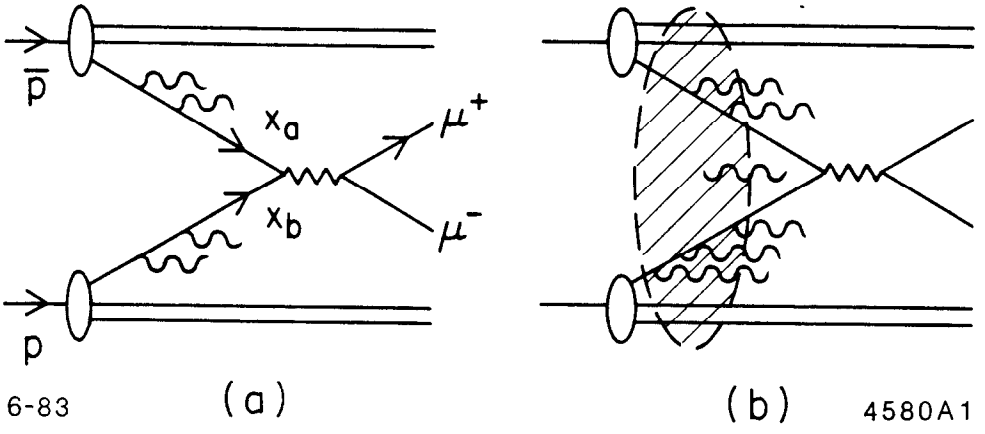

Fig. 1

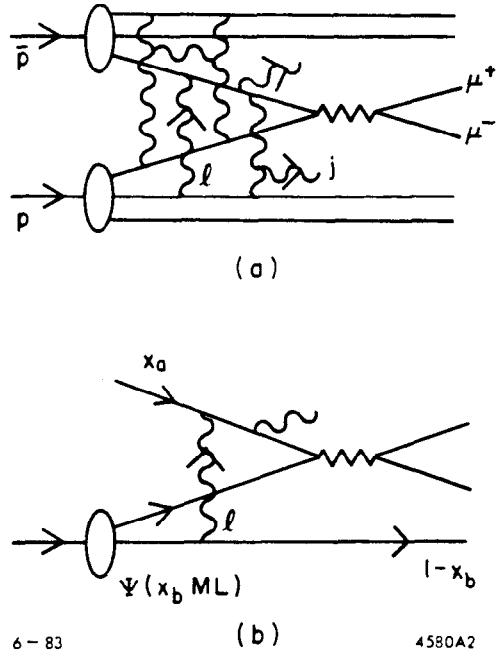

Fig. 2

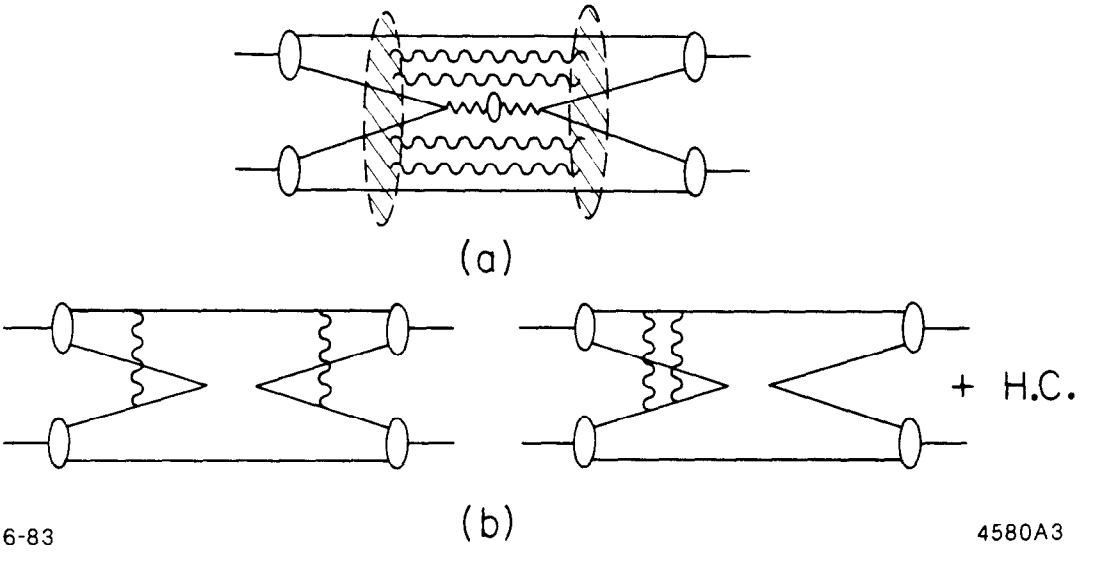

Fig. 3

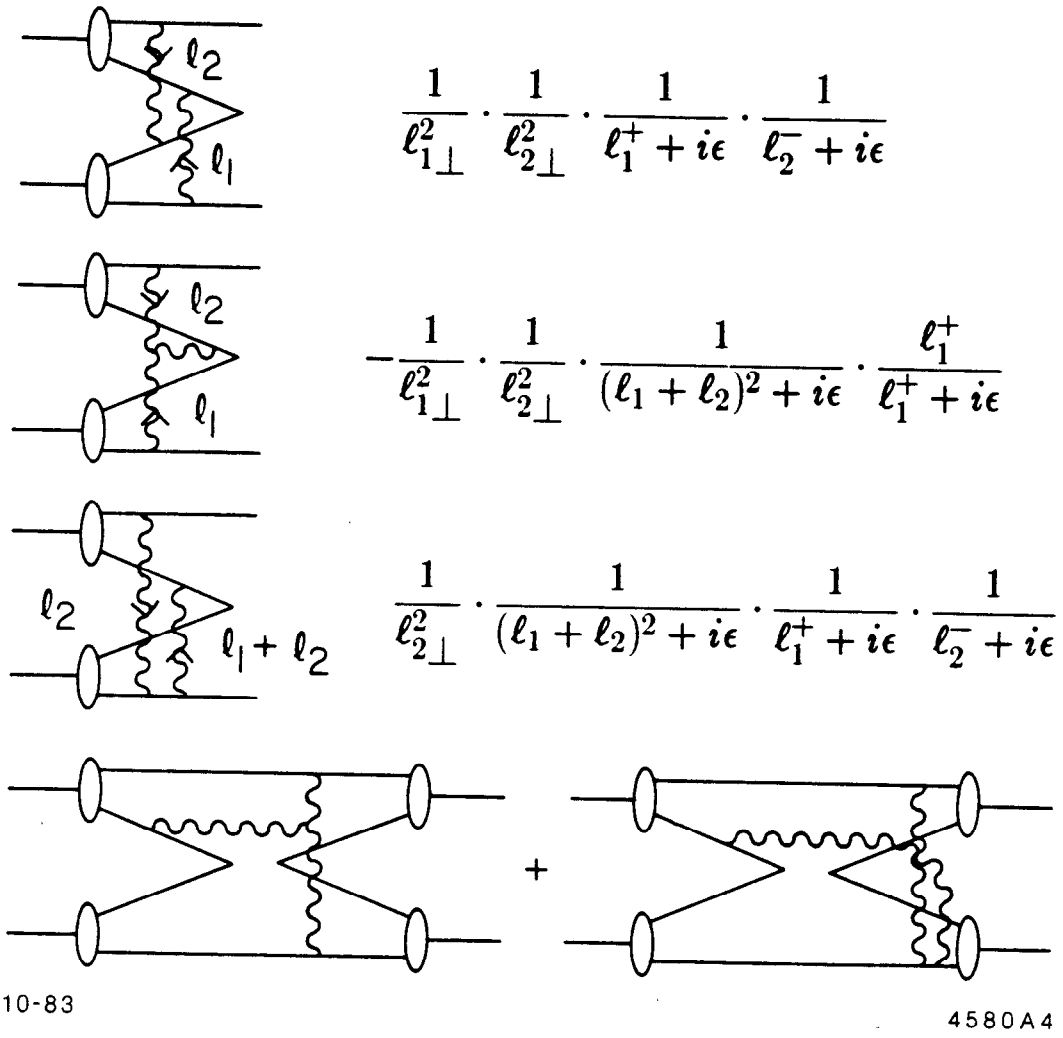
ℓ_2
ℓ_1
$\frac{1}{\ell_{1\perp}^2} \cdot \frac{1}{\ell_{2\perp}^2} \cdot \frac{1}{\ell_1^+ + i\epsilon} \cdot \frac{1}{\ell_2^- + i\epsilon}$
ℓ_2
ℓ_1
$-\frac{1}{\ell_{1\perp}^2} \cdot \frac{1}{\ell_{2\perp}^2} \cdot \frac{1}{(\ell_1 + \ell_2)^2 + i\epsilon} \cdot \frac{\ell_1^+}{\ell_1^+ + i\epsilon}$
ℓ_2
$\ell_1 + \ell_2$
$\frac{1}{\ell_{2\perp}^2} \cdot \frac{1}{(\ell_1 + \ell_2)^2 + i\epsilon} \cdot \frac{1}{\ell_1^+ + i\epsilon} \cdot \frac{1}{\ell_2^- + i\epsilon}$
+
10-83
4580A4

Fig. 4

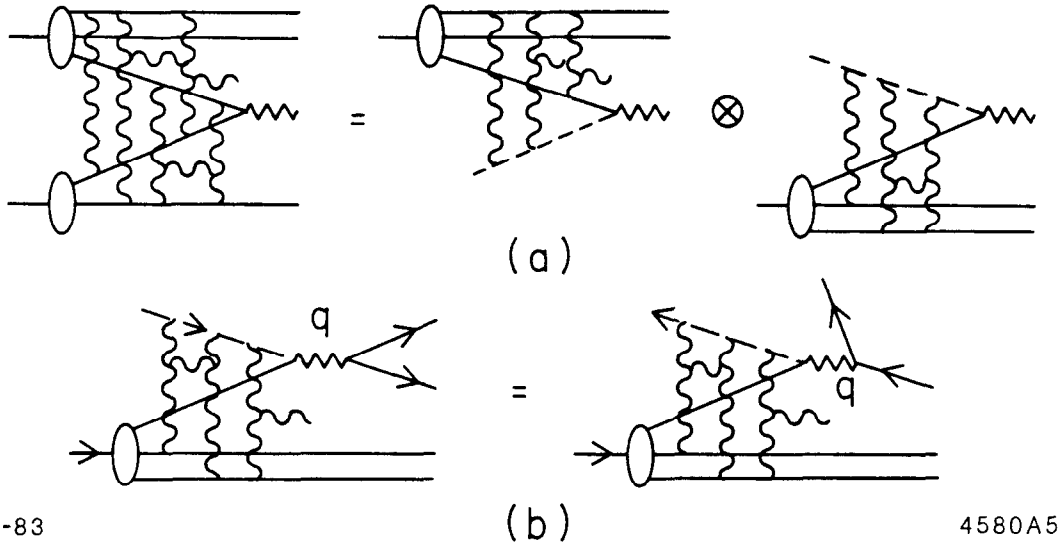

Fig. 5

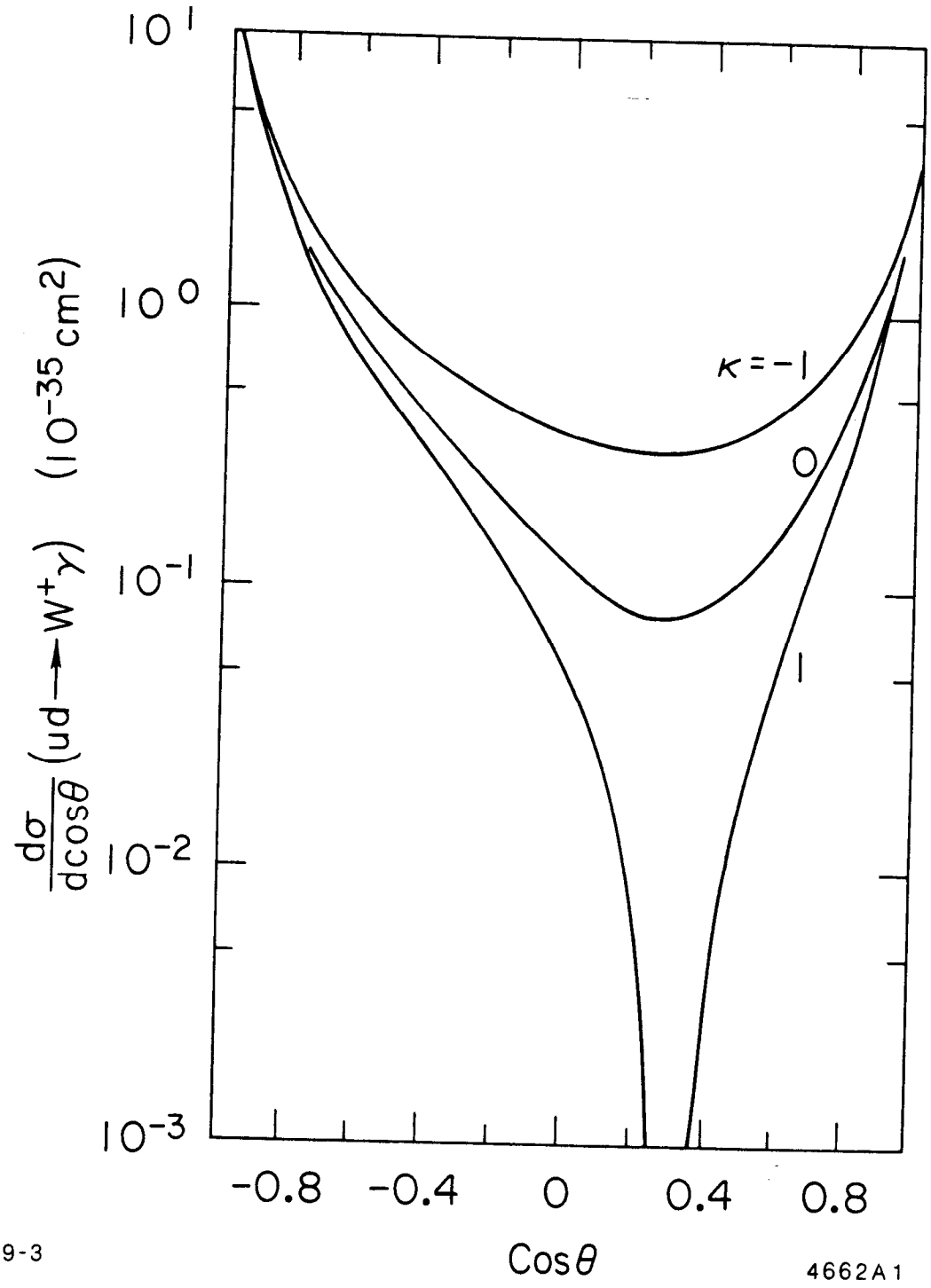
10^1
10^0
10^{-1}
10^{-2}
10^{-3}
$\frac{d\sigma}{d\cos\theta}(ud \rightarrow W^+\gamma)$ $(10^{-35}\,cm^2)$
$\kappa = -1$
0
1
-0.8
-0.4
0
0.4
0.8
$\cos\theta$
9-3
4662A1

Fig. 6

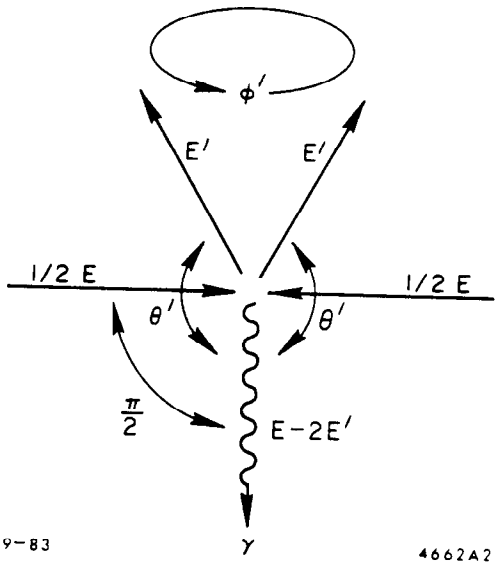

Fig. 7

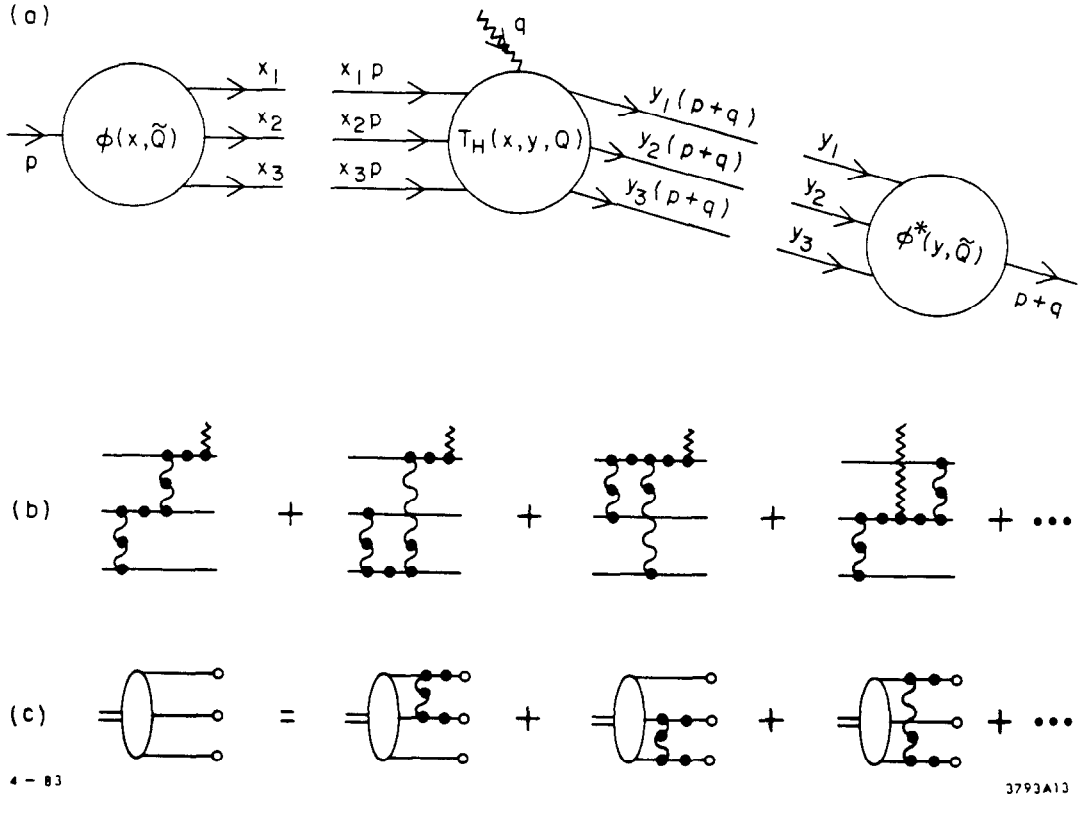
(a)
$\phi(x,\tilde{Q})$
p
x_1
x_2
x_3
q
$x_1 p$
$x_2 p$
$x_3 p$
$T_H(x,y,Q)$
$y_1(p+q)$
$y_2(p+q)$
$y_3(p+q)$
y_1
y_2
y_3
$\phi^*(y,\tilde{Q})$
p+q
(b)
(c)
4-83
3793A13

Fig. 8

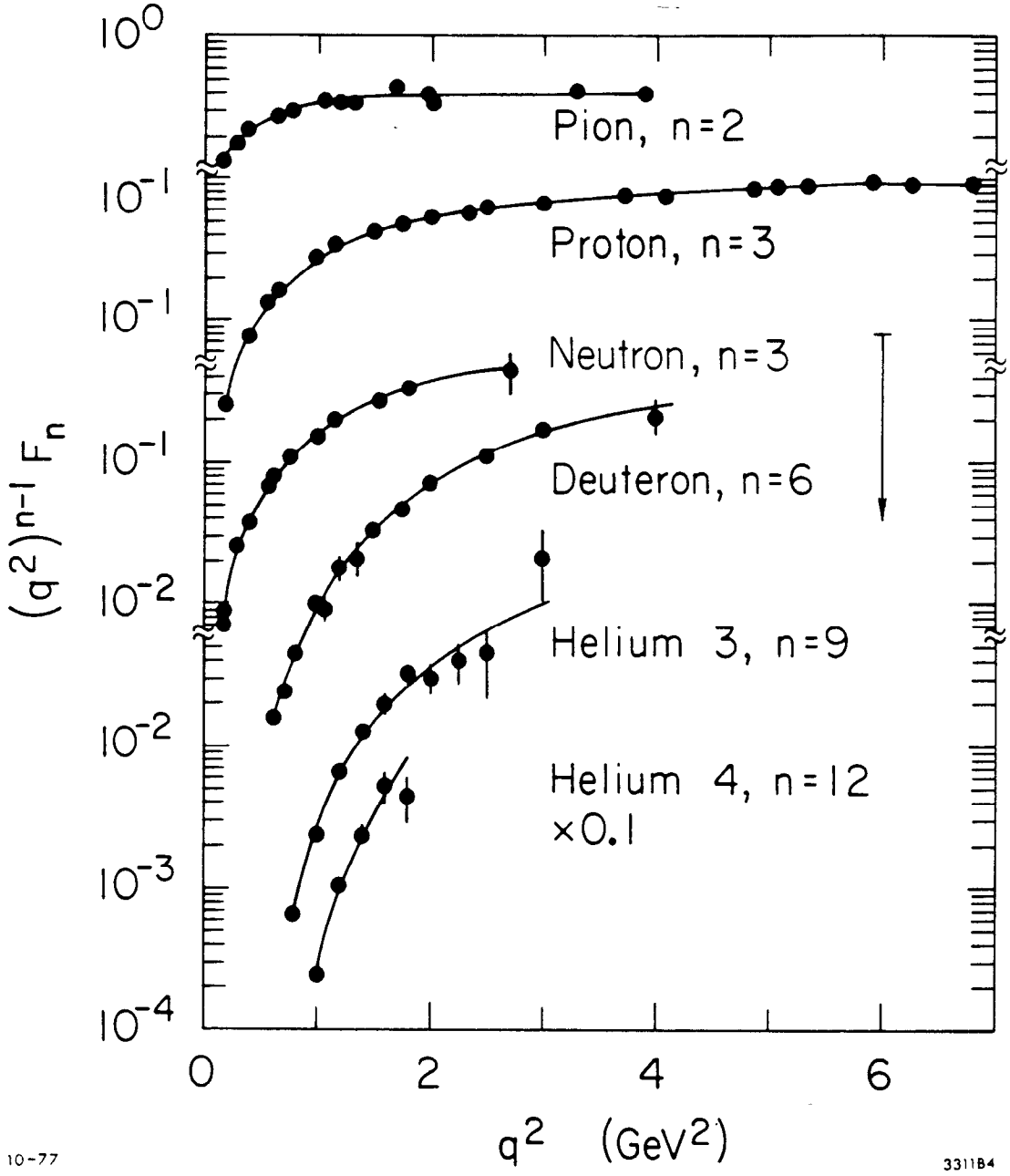
10^0
10^{-1}
10^{-1}
10^{-1}
10^{-2}
10^{-2}
10^{-3}
10^{-4}
$(q^2)^{n-1} F_n$
Pion, n=2
Proton, n=3
Neutron, n=3
Deuteron, n=6
Helium 3, n=9
Helium 4, n=12
×0.1
0
2
4
6
q^2 (GeV^2)
10-77
331184

Fig. 9

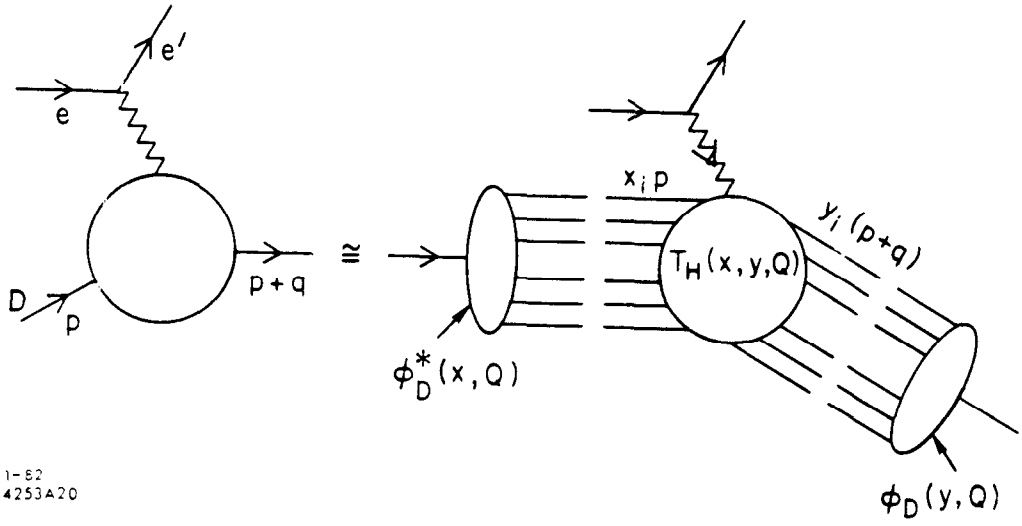

Fig. 10

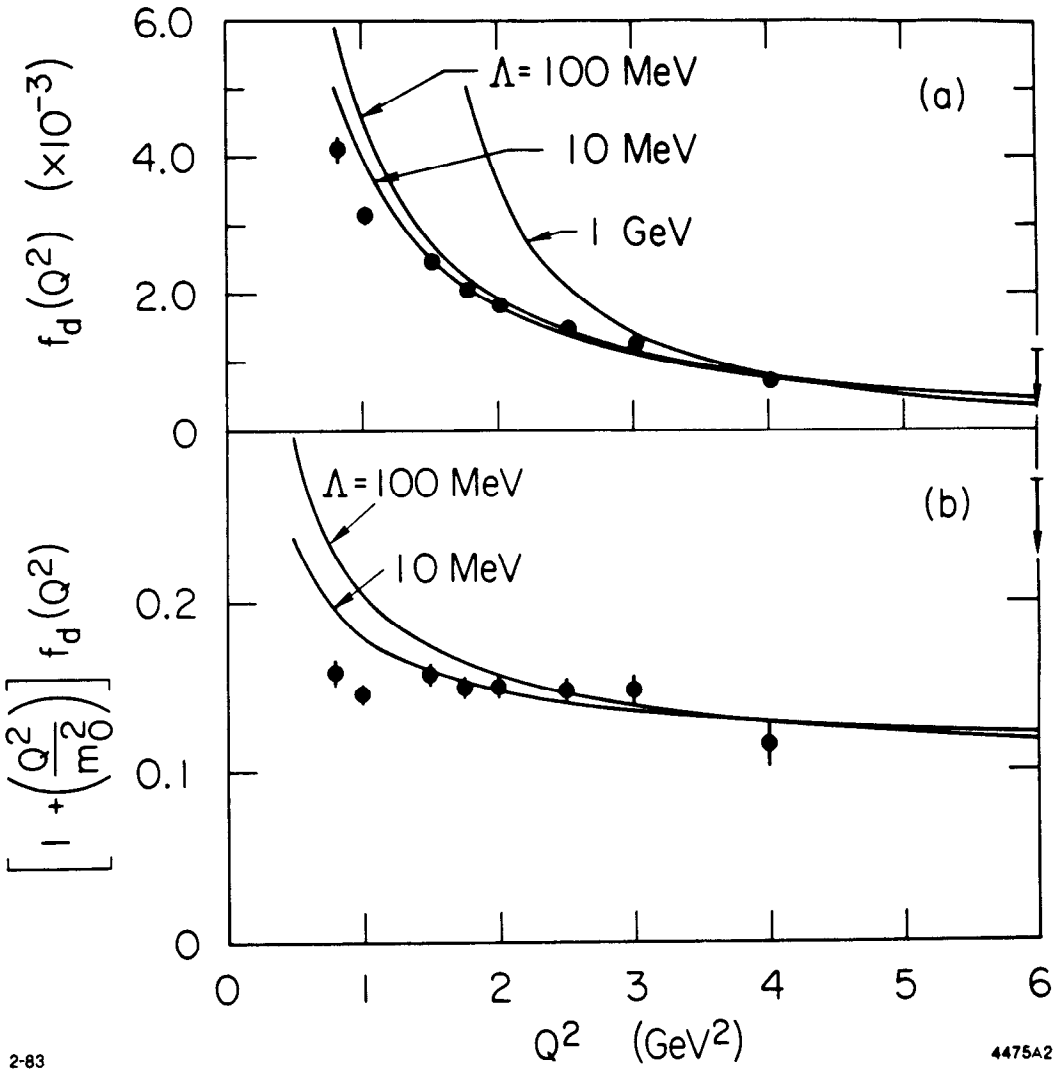
6.0
4.0
2.0
0
$f_d(Q^2)$ $(\times 10^{-3})$
Λ = 100 MeV
10 MeV
1 GeV
(a)
Λ = 100 MeV
10 MeV
(b)
0.2
0.1
0
$\left[1+\left(\frac{Q^2}{m_0^2}\right)\right] f_d(Q^2)$
0
1
2
3
4
5
6
Q^2 (GeV^2)
2-83
4475A2

Fig. 11

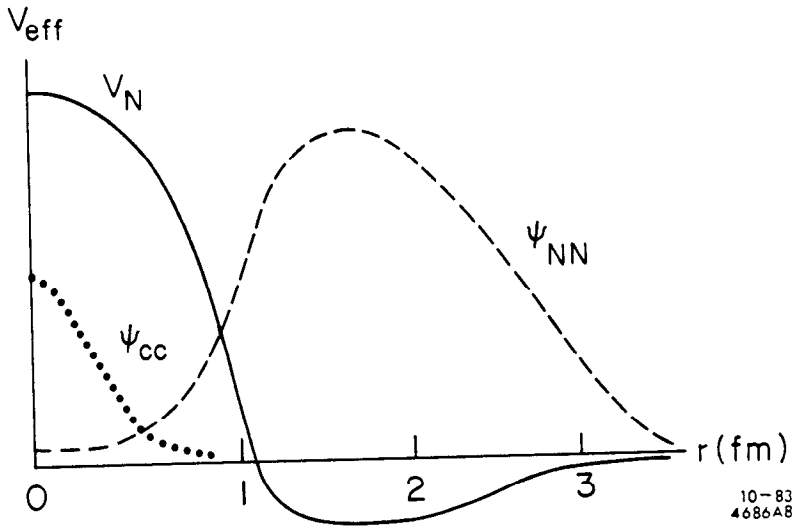

Fig. 12

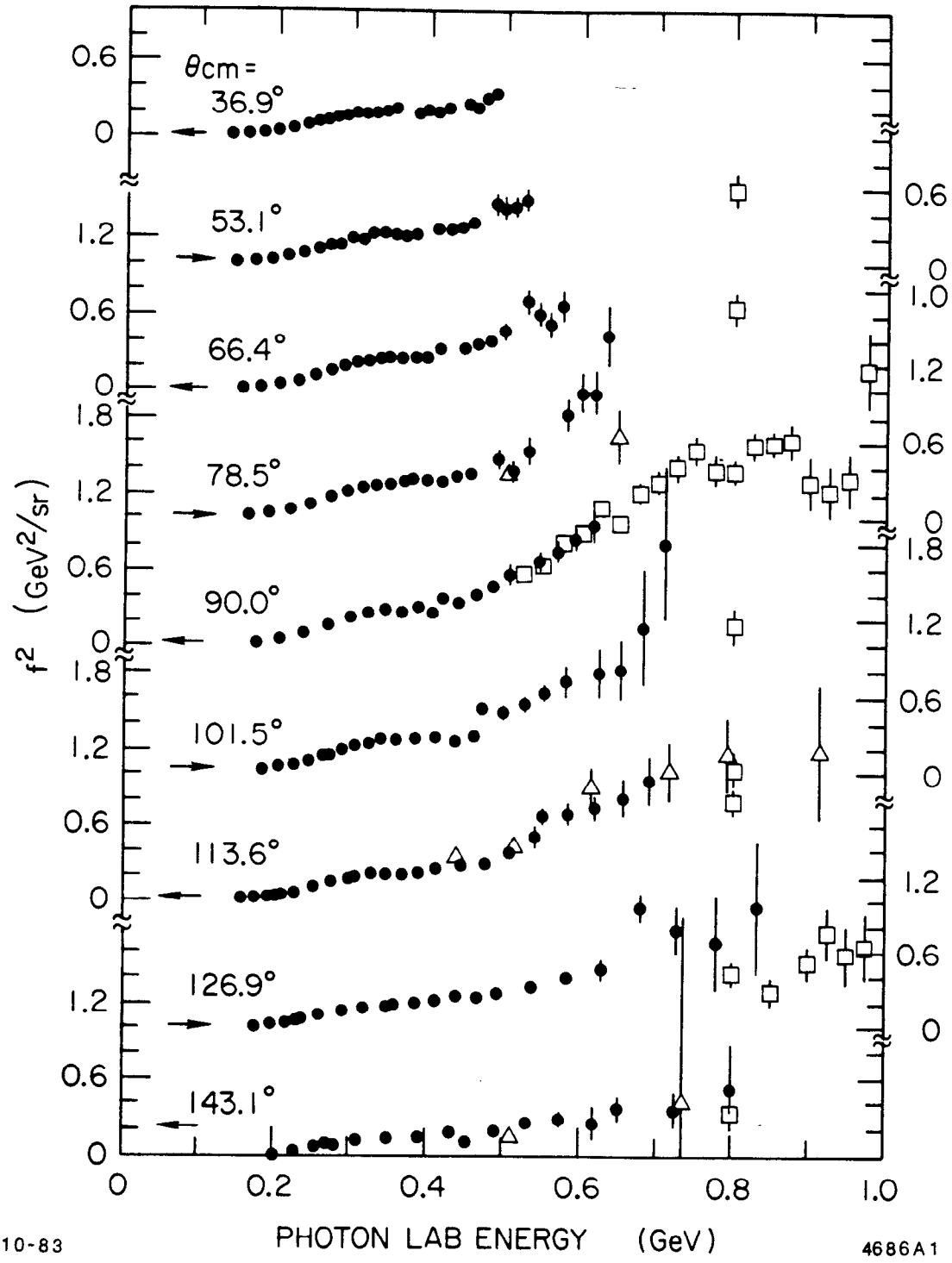
θcm =
36.9°
53.1°
66.4°
78.5°
90.0°
101.5°
113.6°
126.9°
143.1°
f² (GeV²/sr)
PHOTON LAB ENERGY (GeV)
10-83
4686A1

Fig. 13

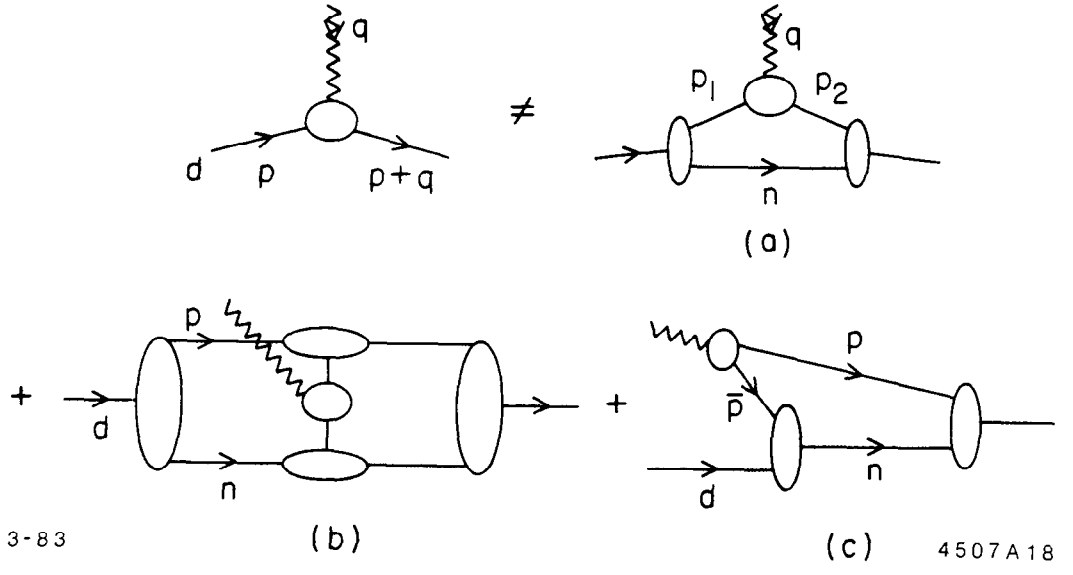

Fig. 14

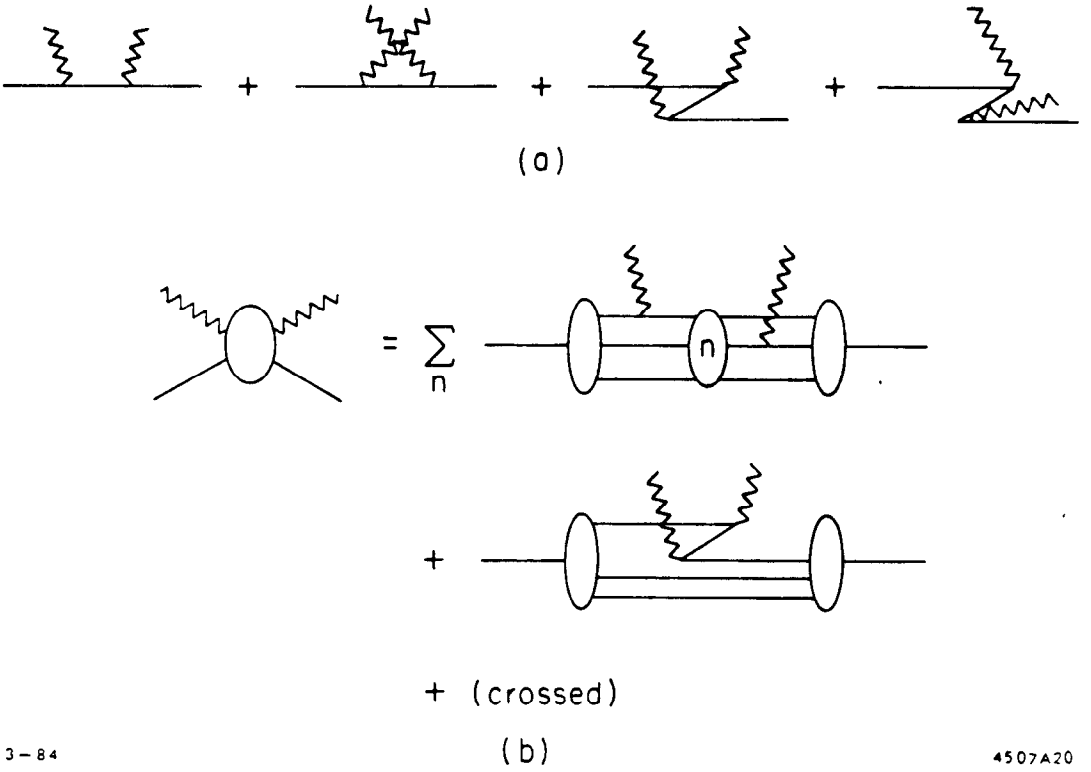

Fig. 15